

# Vision Meets Drones: Past, Present and Future

Pengfei Zhu\*, Longyin Wen\*, Dawei Du\*, Xiao Bian, Qinghua Hu, Haibin Ling

**Abstract**—Drones, or general UAVs, equipped with cameras have been fast deployed with a wide range of applications, including agriculture, aerial photography, and surveillance. Consequently, automatic understanding of visual data collected from drones becomes highly demanding, bringing computer vision and drones more and more closely. To promote and track the developments of object detection and tracking algorithms, we have organized two challenge workshops in conjunction with ECCV 2018, and ICCV 2019, attracting more than 100 teams around the world. We provide a large-scale drone captured dataset, VisDrone, which includes four tracks, *i.e.*, (1) image object detection, (2) video object detection, (3) single object tracking, and (4) multi-object tracking. In this paper, we first presents a thorough review of object detection and tracking datasets and benchmarks, and discuss the challenges of collecting large-scale drone-based object detection and tracking datasets with fully manual annotations. After that, we describe our VisDrone dataset, which is captured over various urban/suburban areas of 14 different cities across China from North to South. Being the largest such dataset ever published, VisDrone enables extensive evaluation and investigation of visual analysis algorithms on the drone platform. We provide a detailed analysis of the current state of the field of large-scale object detection and tracking on drones, and conclude the challenge as well as propose future directions. We expect the benchmark largely boost the research and development in video analysis on drone platforms. All the datasets and experimental results can be downloaded from the website: <https://github.com/VisDrone/VisDrone-Dataset>.

**Index Terms**—Drone, benchmark, image object detection, video object detection, single object tracking, multi-object tracking.



## INTRODUCTION

COMPUTER vision has been attracting increasing amounts of attention in recent years due to its wide range of applications, such as transportation surveillance, smart city, and human-computer interaction. As two fundamental problems in computer vision, object detection and tracking are under extensive investigation. Among many factors and efforts that lead to the fast evolution of computer vision techniques, a notable contribution should be attributed to the invention or organization of numerous benchmarks and challenges, such as Caltech [1], KITTI [2], ImageNet [3], and MS COCO [4] for object detection, and OTB [5], VOT [6], MOTChallenge [7], UA-DETRAC [8], and LaSOT [9] for object tracking.

Drones (or UAVs) equipped with cameras have been fast deployed to a wide range of areas, including agriculture, aerial photography, fast delivery, and surveillance. Consequently, automatic understanding of visual data collected from these drones become highly demanding, which brings computer vision to drones more and more closely. Despite the great progresses in general computer vision algorithms, such as detection and tracking, these algorithms are not usually optimal for dealing with drone captured sequences

or images. This is because of various challenges such as large viewpoint changes and scales. Therefore, it is essential to develop and evaluate new vision algorithms for drone captured visual data. However, as pointed out in [10], [11], studies toward this goal is seriously limited by the lack of publicly available large-scale benchmarks or datasets. Some recent efforts [10], [11], [12] have been devoted to construct datasets captured by drones focusing on object detection or tracking. These datasets are still limited in size and scenarios covered, due to the difficulties in data collection and annotation. Thorough evaluations of existing or newly developed algorithms remain an open problem. A more general and comprehensive benchmark is desired for further boosting video analysis research on drone platforms.

Thus motivated, we have organized two challenge workshops in conjunction with European Conference on Computer Vision (ECCV) 2018, and IEEE International Conference on Computer Vision (ICCV) 2019, attracting more than 100 research teams around the world. The challenge focuses on object detection and tracking with four tracks.

- Pengfei Zhu, Longyin Wen, and Dawei Du contributed equally to this work. The order of names is determined by coin flipping.
- Pengfei Zhu and Qinghua Hu are with the College of Intelligence and Computing, Tianjin University, Tianjin, China (e-mail: {zhupengfei, huqinghua}@tju.edu.cn).
- Longyin Wen is with the JD Finance America Corporation, Mountain View, CA, USA (e-mail: longyin.wen@jd.com).
- Dawei Du is with the Computer Science Department, University at Albany, State University of New York, Albany, NY, USA (e-mail: ddu@albany.edu).
- Xiao Bian is with GE Global Research, Niskayuna, NY, USA (e-mail: xiao.bian@ge.com).
- Haibin Ling is with Stony Brook University, New York, NY, USA (e-mail: haibin.ling@gmail.com).

- *Image object detection track (DET)*. Given a pre-defined set of object classes, *e.g.*, cars and pedestrians, the algorithm is required to detect objects of these classes from individual images taken by drones.
- *Video object detection track (VID)*. Similar to DET, the algorithm is required to detect objects of predefined object classes from videos taken by drones.
- *Single object tracking track (SOT)*. This track aims to estimate the state of a target, indicated in the first frame, across frames in an online manner.
- *Multi-object tracking track (MOT)*. The goal of the track is to track multiple objects, *i.e.*, localize object instances in each video frame and recover their trajectories in video sequences. In the VisDrone-2018 challenge, this track

is divided into two sub-tracks. The first track allows the algorithms to take the provided object detections in each video frame, while the second track is on the other way round. In the VisDrone-2019 challenge, we merge these two sub-tracks, and do not distinguish submitted algorithms according to whether they use the provided object detections in each video frame as input or not.

Notably, in the workshop challenges, we provide a large-scale dataset, which consists of 263 video clips with 179,264 frames and 10,209 static images. The data is recorded by various drone-mounted cameras, diverse in a wide range of aspects including location (taken from 14 different cities in China), environment (urban and rural regions), objects (*e.g.*, pedestrian, vehicles, and bicycles), and density (sparse and crowded scenes). We select 10 categories of objects of frequent interests in drone applications, such as *pedestrians* and *cars*. Altogether we carefully annotate more than 2.5 million bounding boxes of object instances from these categories. Moreover, some important attributes including visibility of the scenes, object category and occlusion, are provided for better data usage. The detailed comparison of the provided drone datasets with other related datasets in object detection and tracking are presented in Table 1.

In this paper, we focus on the VisDrone Challenge in 2018 and 2019, as well as the methods, results, and evaluation protocols of the challenge<sup>1</sup>. The main contributions are summarized as follows. (1) A large-scale benchmark dataset acquired by various drone-mounted cameras is constructed for object detection and tracking tasks, including *DET*, *VID*, *SOT*, and *MOT*. (2) We thoroughly review and discuss the progress in these fields, and summarize the two challenge workshops held in conjunction with ECCV 2018, and ICCV 2019, aiming to promote and track the developments of algorithms. (3) We conclude the challenges in solving object detection and tracking on drone cameras, as well as propose future directions and improvements in related fields.

Notably, this paper extends the summary papers [27], [28], [29], [30], [31], [32], [33] of the VisDrone Challenge in 2018 and 2019. Specifically, it only takes the competition results from the summary papers in these challenges. Besides, we provide an additional `test-dev` set for the aforementioned four tasks, which is used as the default test set for public evaluation. We add detailed analysis and discussions of the competition results and the evaluation results of the state-of-the-art methods on the `test-dev` set. Finally, we discuss and conclude several potential research directions of object detection and tracking on drone captured videos. We expect the benchmark largely boost the research and development in video analysis on drones.

## 2 RELATED WORK

We briefly discuss some prior work in constructing benchmark object detection and tracking datasets, as well as the related challenges in recent conferences.

### 2.1 Generic Object Detection and Tracking Datasets

**Image object detection datasets.** Several image object detection datasets are collected to promote the developments in

related fields. Dollár *et al.* [1] collect the Caltech dataset for pedestrian detection, which is formed by 350,000 annotated bounding boxes with 2,300 pedestrians in approximate 250,000 frames. KITTI [2] is proposed for autonomous driving, including 7,481 images for training and 7,518 images for testing. It is worth mentioning that PASCAL VOC [34], [35] is one of the most popular benchmarks in generic object detection. For example, PASCAL VOC 2007 includes 9,963 images and 24,640 objects with 20 classes, *e.g.*, *person*, *animal*, *vehicle* and *indoor*. The PASCAL VOC 2012 data consists of 11,530 trainval (train+validation) images with 27,450 objects and 6,929 segmentations for the same classes. Following PASCAL VOC, ImageNet [3], [36] scales up more than an order of magnitude in the number of categories and images, *e.g.*, the training data includes 1.2 million images in 1000 object categories. Besides, MS COCO [4] contains more than 328,000 images and 2.5 million object instances in 91 object categories with pixel-level annotations, which is challenging for both image object detection and segmentation.

**Video object detection datasets.** The video object detection task aims to detect objects of different categories in video sequences. In contrast to image object detection, the temporal coherence is a useful cue to improve the performance. To date, various datasets are collected to facilitate the training and testing of methods in such field. In 2015, the ILSVRC challenge [3] open a taster competition “object detection from video”, which contains 30 categories of objects. Wen *et al.* [8], [37], [38] collect the UA-DETRAC dataset focusing on object detection and tracking in traffic surveillance scenarios, including approximate 1.2 million vehicle objects in 140,000 frames. The MOTChallenge team<sup>2</sup> provides annotations of the MOT16 dataset [39], which consists of 14 challenging sequences in unconstrained traffic environments. As another large-scale video object detection dataset, YouTube-Objects dataset [40] is collected from YouTube with the annotations of 9 ~ 24 videos for 10 object classes. Specifically, only 1,258 frames from the overall 720,152 frames are annotated. Kalogeiton *et al.* [41] provide additional bounding-boxes annotations<sup>3</sup> and construct the YouTube-Objects v2.3 dataset, which includes one object instance annotation per frame in the training set, and all instance annotations for the testing set.

**Single object tracking datasets.** In recent years, numerous datasets, *e.g.*, OTB [5], [42], VOT [23], [43], [44], and ALOV [21], have be developed for single object tracking evaluation. The ALOV dataset [21] is collected from YouTube with 64 different kinds of targets, such as face, person, octopus, and can. It consists of 315 sequences with 89,364 frames in total. Wu *et al.* [5], [42] construct the OTB50 and OTB100 datasets, which includes 50 sequences and 100 sequences, respectively. To investigate how color is critical in visual tracking, Liang *et al.* [22] compile a large set of 128 color sequences with ground truth and challenge factor annotations. Li *et al.* [45] propose the NUS-PRO dataset formed by 365 sequences of people and rigid objects, where 150 sequences are annotated with pixel-level labels. Du *et al.* [46] collect the deformable object tracking dataset with 50 sequences in

1. <http://www.aiskyeye.com>.

2. <https://motchallenge.net/>.

3. <http://calvin.inf.ed.ac.uk/datasets/youtube-objects-dataset/>.

TABLE 1: Comparison of the state-of-the-art benchmarks and datasets. Note that, the resolution indicates the maximum resolution of videos/images included in the benchmarks and datasets. ( $1k = 1,000$ )

Image object detection	scenario	#images	categories	avg. #labels/categories	resolution	occlusion labels	year
Caltech Pedestrian [1]	driving	249k	1	347k	640 × 480	✓	2012
KITTI Detection [2]	driving	15.4k	2	80k	1241 × 376	✓	2012
PASCAL VOC2012 [13]	life	22.5k	20	1,373	469 × 387	✓	2012
ImageNet Object Detection [3]	life	456.2k	200	2,007	482 × 415	✓	2013
MS COCO [4]	life	328.0k	91	27.5k	640 × 640		2014
VEDAI [14]	satellite	1.2k	9	733	1024 × 1024		2015
COWC [15]	aerial	32.7k	1	32.7k	2048 × 2048		2016
CARPK [11]	drone	1,448	1	89.8k	1280 × 720		2017
DOTA [16]	aerial	2,806	15	12.6k	12029 × 5014		2018
<b>VisDrone</b>	drone	10,209	10	54.2k	2000 × 1500	✓	2018

Video object detection	scenario	#frames	categories	avg. #labels/categories	resolution	occlusion labels	year
ImageNet Video Detection [3]	life	2017.6k	30	66.8k	1280 × 1080	✓	2015
UA-DETRAC Detection [8]	surveillance	140.1k	4	302.5k	960 × 540	✓	2015
MOT17Det [17]	life	11.2k	1	392.8k	1920 × 1080	✓	2017
Okutama-Action [18]	drone	77.4k	1	422.1k	3840 × 2160		2017
UAVDT-DET [19]	drone	40.7k	3	267.6k	1080 × 540	✓	2018
DroneSURF [20]	drone	411.5k	1	786.8k	-		2019
<b>VisDrone</b>	drone	40.0k	10	183.3k	3840 × 2160	✓	2018

Single object tracking	scenarios	#sequences	#frames	year
ALOV300 [21]	life	315	89.4k	2014
OTB100 [5]	life	100	59.0k	2015
TC128 [22]	life	128	55.3k	2015
VOT2016 [23]	life	60	21.5k	2016
UAV123 [10]	drone	123	110k	2016
NfS [24]	life	100	383k	2017
DTB70 [24]	drone	70	15.8k	2017
POT 210 [25]	planar objects	210	105.2k	2018
UAVDT-SOT [19]	drone	50	37.2k	2018
<b>VisDrone</b>	drone	167	139.3k	2018

Multi-object tracking	scenario	#frames	categories	avg. #labels/categories	resolution	occlusion labels	year
KITTI Tracking [2]	driving	19.1k	5	19.0k	1392 × 512	✓	2013
MOTChallenge 2015 [7]	surveillance	11.3k	1	101.3k	1920 × 1080		2015
UA-DETRAC Tracking [8]	surveillance	140.1k	4	302.5k	960 × 540	✓	2015
DukeMTMC [26]	surveillance	2852.2k	1	4077.1k	1920 × 1080		2016
Campus [12]	drone	929.5k	6	1769.4k	1417 × 2019		2016
MOT17 [17]	surveillance	11.2k	1	392.8k	1920 × 1080		2017
UAVDT-MOT [19]	drone	40.7k	3	267.6k	1080 × 540	✓	2018
<b>VisDrone</b>	drone	40.0k	10	183.3k	3840 × 2160	✓	2018

unconstrained environments. Galoogahi *et al.* [24] propose the Need for Speed (NfS) dataset with 100 sequences formed by 380,000 frames, which is captured with now commonly available higher frame rate (240 FPS) cameras from real world scenarios. To advance the developments of visual tracking algorithms, Kristan *et al.* [23], [44] organize the VOT competition from 2013 to 2020. In addition to VOT, Felsberg *et al.* [47], [48] organize the VOT-TIR competition from 2015 to 2017, focusing on object tracking on thermal infrared sequences.

**Multi-object tracking datasets.** PETS09 [49] is one of the pioneer multi-object tracking datasets, collected from several crowd scenarios. Following PETS09 [49], various multi-object tracking datasets are developed, including KITTI [2], MOTChallenge [7], [39], and UA-DETRAC [8], [37], [38]. The KITTI tracking dataset [2] is designed for autonomous driving, including 21 training and 29 testing sequences. The MOTChallenge team establishes a unified platform to evaluate multi-pedestrian tracking methods, including the MOT15 [7] (22 sequences) and MOT16 [39] (14 sequences) datasets. The UA-DETRAC dataset [8], [37], [38] is collected in traffic scenarios, which includes 100 sequences for multi-vehicle tracking.

Moreover, some datasets are developed for evaluating multi-camera multi-object tracking methods. Ferryman and Shahrokni [49] collect a dataset using multi-camera with fully overlapping views in constrained environments. Some

other datasets focus on multi-object tracking on multiple non-overlapping cameras. Chen *et al.* [50] construct 4 datasets. Each of them are recorded by 3 to 5 cameras with non-overlapping views in real-world scenarios and simulation environments. Zhang *et al.* [51] develop a dataset composed of 5 to 8 cameras covering both indoor and outdoor scenes in the university scene. Ristani *et al.* [26] organize a challenge and provide a large-scale fully-annotated and calibrated dataset, including more than 2 million  $1080 \times 1920$  video frames taken by 8 cameras with more than 2,700 object identities.

## 2.2 Drone-based Datasets

To date, there only exist a handful of drone-captured datasets in computer vision field. Hsieh *et al.* [11] present a dataset for car counting, which consists of 1,448 images captured in parking lot scenarios with the drone platform, including 89,777 annotated cars. Robicquet *et al.* [12] collect several video sequences with the drone platform in campuses, including various types of objects, (*i.e.*, pedestrians, bikes, skateboarders, cars, buses, and golf carts), which enable the design of new object tracking and trajectory forecasting algorithms. Barekatin [18] present a new Okutama-Action dataset for concurrent human action detection with the aerial view. The dataset includes 43 minute-long fully-annotated sequences with 12 action classes. In [10], a high-resolution UAV123 dataset is presented for single object

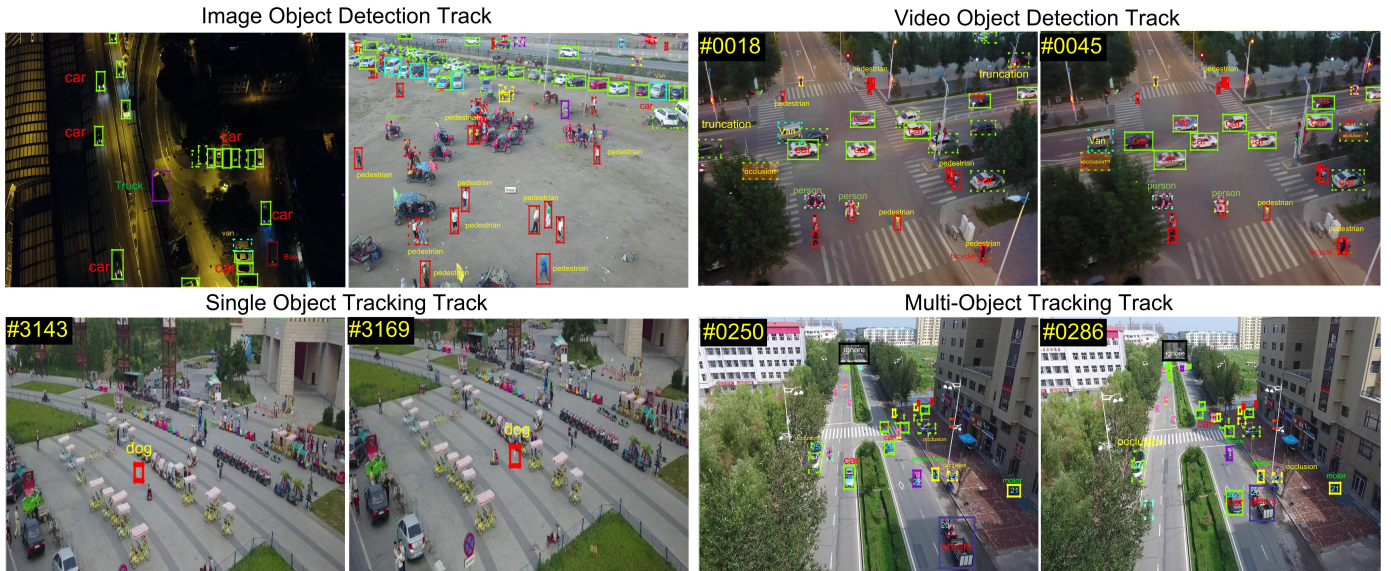


Fig. 1: Some annotated example images of the proposed datasets. The dashed bounding box indicates the object is occluded. Different bounding box colors indicate different classes of objects. For better visualization, we only display some attributes.

tracking, which contains 123 aerial video sequences with 110,000 fully annotated frames, including the bounding boxes of people and their corresponding action labels. Li *et al.* [52] capture 70 video sequences of high diversity by drone cameras and manually annotate the bounding boxes of objects for single object tracking evaluation. Moreover, Du *et al.* [19] construct a new UAV benchmark focusing on complex scenarios for three tasks including object detection, single object tracking, and multiple object tracking. In [53], Rozantsev *et al.* present two separate datasets for detecting flying objects, *i.e.*, the UAV dataset and the aircraft dataset. The former one comprises 20 video sequences with the resolution  $752 \times 480$  and 8,000 annotated bounding boxes of objects, acquired by a camera mounted on a drone flying indoors and outdoors. The latter one consists of 20 publicly available videos of radio-controlled planes with 4,000 annotated bounding boxes. Recently, Xia *et al.* [16] propose a large-scale dataset in aerial images collected from different sensors and platforms to advance object detection research in earth vision. In contrast to the aforementioned datasets acquired in constrained scenarios for object tracking, detection and counting, our **VisDrone** dataset is captured in various unconstrained scenes, focusing on four core problems in computer vision fields, *i.e.*, image object detection, video object detection, single object tracking, and multi-object tracking.

### 2.3 Existing Challenges

The international workshop on computer vision for UAVs<sup>4</sup> focuses on hardware, software and algorithmic (co-)optimizations towards state-of-the-art image processing on UAVs. The VOT challenge workshop<sup>5</sup> provides the tracking community with a precisely defined and repeatable way to compare short-term trackers as well as provides a common platform for discussing the evaluation and advancements

made in the field of single-object tracking. The BMTT and BMTT-PETS workshops<sup>6</sup> aims to pave the way for a unified framework towards more meaningful quantification of multi-object tracking. The PASCAL VOC challenge has been held for eight years from 2005 to 2012, which aims to recognize objects from a number of visual object classes in realistic scenes. The ILSVRC challenge also has been held for eight years from 2010 to 2017, which is designed to evaluate algorithms for object detection and image classification at large scale. Compared to the aforementioned challenges, our workshop challenge focuses on object detection and tracking on drones with the following four tracks: (1) image object detection, (2) video object detection, (3) single object tracking, and (4) multi-object tracking. Our goal is to develop and distribute a new challenging benchmark for real world problems on drones with new difficulties, *e.g.*, large scale and viewpoint variations, and heavy occlusions.

## 3 VISDRONE OVERVIEW

A critical basis for effective algorithm evaluation is a comprehensive dataset. For this purpose, in **VisDrone**, we systematically collected the largest VisDrone benchmark dataset to advance the object detection and tracking research on drones. It consists of 263 video clips with 179,264 frames and additional 10,209 static images. The videos/images are acquired by various drone platforms, *i.e.*, DJI Mavic, Phantom series (3, 3A, 3SE, 3P, 4, 4A, 4P), including different scenarios across 14 different cities in China, *i.e.*, Tianjin, Hongkong, Daqing, Ganzhou, Guangzhou, Jincang, Liuzhou, Nanjing, Shaoxing, Shenyang, Nanyang, Zhangjiakou, Suzhou and Xuzhou. The dataset covers various weather and lighting conditions, representing diverse scenarios in our daily life. The maximal resolutions of video clips and static images are  $3840 \times 2160$  and  $2000 \times 1500$ , respectively.

4. <https://sites.google.com/site/uavision2018/>.

5. <http://www.votchallenge.net/vot2019/>.

6. <https://motchallenge.net/>.

The VisDrone benchmark focuses on the following four tasks (see Fig. 1), *i.e.*, (1) image object detection, (2) video object detection, (3) single-object tracking, and (4) multi-object tracking. We construct a website: [www.aiskyeye.com](http://www.aiskyeye.com) for accessing the **VisDrone** dataset and perform evaluation of those four tasks. Notably, for each task, the images/videos in the training, validation, and testing subsets are captured at different locations, but share similar scenarios and attributes. The training subset is used to train the algorithms, the validation subset is used to validate the performance of algorithms, the test-challenge subset is used for workshop competition, and the test-dev subset is used as the default test set for public evaluation. The manually annotated ground-truths for training and validation subsets are made available to participants, but the ground-truths of the testing subset are reserved in order to avoid (over)fitting of algorithms.

To participate our challenge, research teams are required to create their own accounts using the institutional email address. After registration, participants can choose the tasks of interest, and submit the results specifying locations or trajectories of objects in the images or videos using the corresponding accounts. The participants are encouraged to use the provided training data, but additional training data is allowable after declaration in submission. In the following subsections, we describe the data statistics and annotation of the datasets for each track in detail.

## 4 DET TRACK

The *DET* track tackles the problem of localizing multiple object categories in the image. For each image, algorithms are required to locate all the object instances of predefined set of object categories, *e.g.*, car and pedestrian, in a given input images (if any). That is, we require the detection algorithm to predict the bounding box of each instance of each object class in the image, with a real-valued confidence. We mainly focus on ten object categories in evaluation, including *pedestrian*, *person*<sup>7</sup>, *car*, *van*, *bus*, *truck*, *motor*, *bicycle*, *awning-tricycle*, and *tricycle*. Some rarely occurring vehicles (*e.g.*, machinshop truck, forklift truck, and tanker) are ignored in evaluation. The performance of algorithms is evaluated by the *average precision* (AP) across different object categories and intersection over union (IoU) thresholds.

### 4.1 Data Collection and Annotation

The *DET* dataset consists of 10,209 images in unconstrained challenging scenes, including 6,471 images in the training subset, 548 in the validation subset, 1,580 in the test-challenge subset, and 1,610 in the test-dev subset. We plot percentage of the number of objects per image in Fig. 2 and the number of objects in different object categories with different occlusion degrees in Fig. 3. Notably, the large variations of the number of objects in each image and the class imbalance issue significantly challenge the performance of detection algorithms. For example, as shown in Fig. 2, the minimal and maximal numbers of objects in the test-challenge subsets are 0 and 364, and

<sup>7</sup> If a human maintains standing pose or walking, we classify it as *pedestrian*; otherwise, it is classified as a *person*.

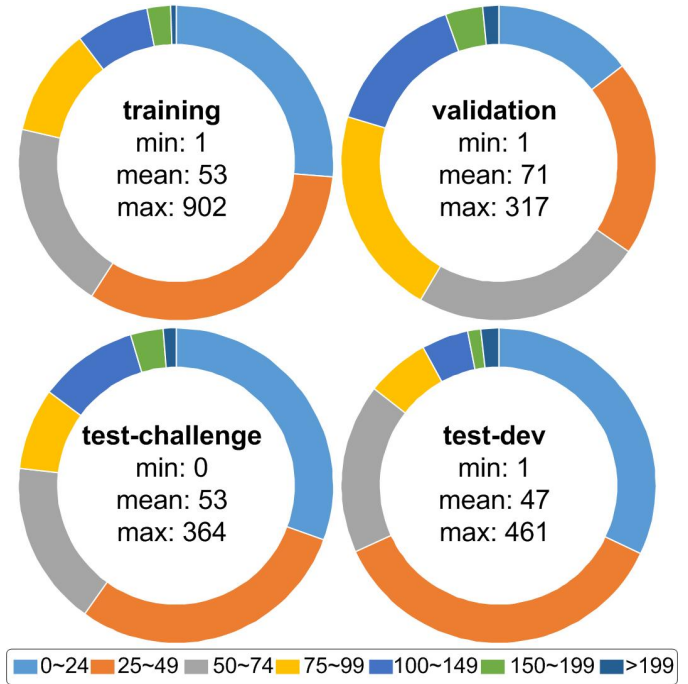


Fig. 2: Percentage of the number of objects per image in the training, validation, test-challenge and test-dev subsets in the *DET* track.

the number of the *awning-tricycle* instances is more than  $40\times$  less than the *car* instances.

In this track, we focus on people and vehicles in our daily life, and define 10 object categories of interest including *pedestrian*, *person*, *car*, *van*, *bus*, *truck*, *motor*, *bicycle*, *awning-tricycle*, and *tricycle*, in evaluation. Some rarely occurring vehicles (*e.g.*, machinshop truck, forklift truck, and tanker) are ignored in evaluation. We manually annotate the bounding boxes of different categories of objects in each image. After that, cross-checking is conducted to ensure annotation quality. Moreover, we also provide two attributes of each annotated bounding box to analyze the algorithms thoroughly, *i.e.*, the *occlusion* and *truncation* ratios. Specifically, occlusion ratio  $\alpha$  denotes the fraction of objects being occluded by other objects or background, including no occlusion ( $\delta = 0\%$ ), partial occlusion ( $\delta \in (0\%, 50\%]$ ), and heavy occlusion ( $\delta \in (50\%, 100\%]$ ). Truncation ratio denotes the degree of object parts appearing outside a frame when the object is captured near the frame boundary. It is computed based on the region outside the frame by human. Notably, the object instance is not considered in evaluation if the truncation ratio is larger than 50%.

### 4.2 Evaluation Protocol

For the *DET* track, the algorithm is required to output detected bounding boxes with confidence scores in each image. Similar to the metrics in the MS COCO benchmark [4], we evaluate detectors by the  $AP^{IoU=0.50:0.05:0.95}$ ,  $AP^{IoU=0.50}$ ,  $AP^{IoU=0.75}$ ,  $AR^{max=1}$ ,  $AR^{max=10}$ ,  $AR^{max=100}$  and  $AR^{max=500}$  scores, which penalizes missing detections and false alarms. Specifically,  $AP^{IoU=0.50:0.05:0.95}$  is computed by averaging over all 10 intersection over union (IoU) thresholds (*i.e.*, in the range  $[0.50 : 0.95]$  with uniform step size 0.05) of all

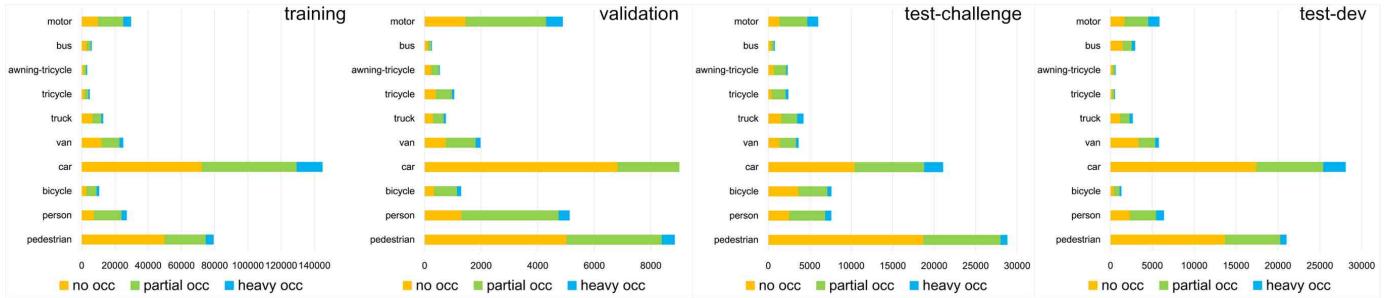


Fig. 3: The number of objects with different occlusion degrees of different object categories in the training, validation, test-challenge and test-dev sets in the DET track.

categories, which is used as the primary metric for ranking.  $AP^{IoU=0.50}$  and  $AP^{IoU=0.75}$  are computed at the single IoU thresholds 0.5 and 0.75 over all categories, respectively. The  $AR^{max=1}$ ,  $AR^{max=10}$ , and  $AR^{max=100}$  scores are the maximum recalls given 1, 10, 100 and 500 detections per image, averaged over all categories and IoU thresholds. Please refer to [4] for more details.

### 4.3 Brief Review of DET Algorithms

Early object detection algorithms are built on well-defined hand-crafted features and classifiers, including Adaboost [73], HOG [74], DPM [75], ACF [76] and ICF [77]. With the arrival of deep convolutional network, object detection field is quickly dominated by the CNN-based methods. such as R-CNN [78], SPPNet [79], Fast R-CNN [80], Faster R-CNN [55], Mask R-CNN [81], and Cascade R-CNN [61]. To avoid computationally expensive region proposal generation in the aforementioned methods, some methods directly predict object classes and bounding box offsets using a single feed-forward CNN, such as YOLO [60], [82], [83], SSD [56], and RefineDet [62]. In recent years, some researchers (*e.g.*, CornerNet [84], CenterNet [64], FCOS [85] and FSAF [86]) leverage deep networks to determine the center location and scale of objects without paving pre-defined anchors, further improving the state-of-the-arts in several public datasets.

### 4.4 Submitted Algorithms

**VisDrone 2018 challenge.** There are 34 different object detection algorithms from 31 different institutes submitted to this track [27]. We present the results and team information in Table 2. As shown in Table 2, several methods are constructed based on the Faster R-CNN algorithm [55], such as CERTH-ODI, DPNNet, Faster R-CNN+, Faster R-CNN2, Faster R-CNN3, IITH DODO, JNU\_Faster R-CNN, MFaster R-CNN, and MMN. Some algorithms construct feature pyramids to build high-level semantic feature maps at all scales, including DE-FPN, DFS, FPN+, FPN2, FPN3, and DDFPN. 5 detectors, *i.e.*, MSYOLO, SODLSY, YOLOv3+, YOLOv3++ and YOLOv3\_DP, are improved from the one-stage YOLOv3 method [60]. MMF and YOLO-R-CNN fuse multi-models of the Faster R-CNN and YOLOv3 methods. Keras-RetinaNet, RetinaNet2 and HAL-Retina-Net are based on RetinaNet [57]. RD<sup>4</sup>MS, RefineDet+ and R-SSRN are based on the RefineDet method [62]. The top accuracy is achieved by the HAL-Retina-Net method, *i.e.*, 31.88

AP, which uses the SE module [87] and downsampling-upsampling operations [88] to learn both the channel and spatial attentions.

**VisDrone 2019 challenge.** We have received 47 detection methods from 27 different institutes in this track [28], shown in Table 2. 9 methods are improved from Cascade R-CNN [61], *i.e.*, Airia-GA-Cascade, Cascade R-CNN+, Cascade R-CNN++, DCRCNN, DPN, DPNNet-ensemble, MSCRDet, SAMFR-Cascade RCNN and SGE-cascade R-CNN. 6 detection methods, *i.e.*, CenterNet, CenterNet-Hourglass, CN-DhVaSa, ConstraintNet, GravityNet and RRNet, are based on the anchor-free method CenterNet [64]. 5 detection methods, *i.e.*, DA-RetinaNet, EHR-RetinaNet, FS-Retinanet, MOD-RETINANET and retinaplus, are improved from the anchor-based method RetinaNet [57]. ACM-OD, BetterFPN and ODAC construct multi-scale feature pyramids using FPN [58]. CNAnet designs the convolution neighbor aggregation mechanism for detection. HRDet+ is improved from HRDet [66], which connects the convolutions from high to low resolutions in parallel to generate discriminative high-resolution representations. TridentNet [71] generates scale-specific feature using a parallel multi-branch architecture.

Some other methods use ensemble mechanism to improve the performance. DPNNet-ensemble achieves the top accuracy with 29.62% AP, which ensembles two object detectors based on Cascade R-CNN [61] using ResNet-50 and ResNet-101 as feature extractors with global context module [89] and deformable convolution [90]. EnDet combines the results of YOLOv3 [60] and Faster R-CNN [55]. TSEN ensembles three two-stage methods including Faster R-CNN [55], Guided Anchoring [72] and Libra R-CNN [69]. ERCNNs combines the results of Cascade R-CNN [61] and Faster R-CNN [55] with different kinds of backbones. Libra-HBR ensembles the improved SNIPER [68], Libra R-CNN [69] and Cascade R-CNN [61].

To further improve the accuracy, some methods jointly predict the masks and bounding boxes of objects. For example, DBCL [65] uses the bounding box annotations to train a segmentation model to produce accurate results. HTC-drone improves the hybrid task cascade algorithm [67] using the instance segmentation cascade. The S+D method is formed by the segmentation algorithm DeepLab [70] and the detection module in HRDet [66].

**VisDrone-dev benchmark.** This benchmark is designed for public evaluation. 7 state-of-the-art object detection methods are evaluated, *i.e.*, FPN [58], RetinaNet [57], Light-

TABLE 2: Teams participating in the VisDrone-DET 2018 and 2019 challenges, ordered alphabetically.

CodeName	AP	Institutions	Contributions and References
VisDrone-2018 Challenge:			
AHOD	12.77	Tsinghua Univ.	J. Wang, Y. Li, S. Wang [54]
CERTH-ODI	5.04	ITI Tech. College	E. Michail, K. Avgerinakis, P. Giannakeris, S. Vrochidis, I. Kompatsiaris [55]
CFE-SSDv2	26.48	Peking Univ.	Q. Zhao, F. Ni, Y. Wang [56]
DDFPN	21.05	Tianjin Univ.	L. Lu [57]
DE-FPN	27.10	South China Univ. of Tech.	J. Zhou, Y. Luo, H. Lin, Q. Liu [58]
DFS	16.73	SUN YAT-SEN Univ.	K. Bo [58]
DPNet	30.92	Univ. of Elec. Sci. & Tech. of China	H. Li, Qishang Cheng, Wei Li, X. Chen, H. Qiu, Z. Song [55]
Faster R-CNN+	9.67	Shandong Univ.	T. Lee, Y. Fan, H. Deng, L. Ma, W. Zhang [55]
Faster R-CNN2	21.34	Xidian Univ.	F. Zhang [55]
Faster R-CNN3	3.65	Northwestern Poly. Univ.	Y. Liu, Y. Li [55]
FPN+	13.32	Texas A&M Univ.*, IBM <sup>†</sup>	K. Suresh*, H. Xu*, N. Bansal*, C. Brown*, Y. Wei*, Z. Wang*, H. Shi <sup>†</sup> [58]
FPN2	16.15	Chongqing Univ.	Z. He, L. Zhang [58]
FPN3	13.94	Nanjing Univ. of Sci. and Tech.	C. Li, Z. Cui [58]
HAL-Retina-Net	<b>31.88</b>	Tsinghua Univ.	Y. Li, Z. Xia, S. Wang [57]
IITH DODO	14.04	IIT Hyderabad	N. Mangain, N. Vedurupaka, K. Joseph, V. Balasubramanian [55]
JNU_Faster RCNN	8.72	Jiangnan Univ.	H. Zhang [55]
Keras-RetinaNet	7.72	Xidian Univ.	Q. Sun, S. Jiang [57]
L-H RCNN+	21.34	Xidian Univ.	L. Yang, Q. Wang, L. Cheng, S. Wei [59]
MFaster-RCNN	18.08	Beijing Univ. of Posts and Telecom.	W. He, F. Zhu [55]
MMF	7.54	Xiamen Univ.	Y. Zhang, W. Wu, Z. Guo, M. Huang [55], [60]
MMN	10.40	Ocean Univ. of China	X. Sun [55]
MSCNN	2.89	National Univ. of Defense Tech.	D. Li, Y. Kuai, H. Liu, Z. Deng, J. Zhao [61]
MSYOLO	16.89	Xidian Univ.	H. Wang, Z. Wang, K. Wang, X. Li [60]
RD <sup>4</sup> MS	22.68	Fraunhofer IOSB	O. Acatay, L. Sommer, A. Schumann [62]
RefineDet+	21.07	Univ. of Chinese Acad. of Sci.	K. Duan, H. Qi, Q. Huang [62]
RetinaNet2	5.21	Xidian Univ.	L. Yang, Q. Wang, L. Cheng, S. Wei [57]
R-SSRN	9.49	Xidian Univ.	W. Yang, J. Yang [62]
SOD	8.27	Shanghai Jiao Tong Univ.*, Univ. of Ottawa <sup>†</sup>	L. Ding*, Y. Wang <sup>†</sup> , C. Qian*, R. Laganière <sup>†</sup> , X. Luo* [63]
SODLSY	13.61	National Lab. of Pattern Recognition	S. Wang, Y. Zhang, J. Cheng [60]
YOLO-R-CNN	12.06	Univ. of Kansas	W. Ma, Y. Wu, U. Sajid, G. Wang [55], [60]
YOLOv3+	15.26	Xidian Univ.	S. Wang, X. Lian [60]
YOLOv3++	10.25	Univ. of Kansas	Y. Wu, W. Ma, U. Sajid, G. Wang [60]
YOLOv3_DP	20.03	Xidian Univ.	Q. Sun, S. Jiang [60]
VisDrone-2019 Challenge:			
ACM-OD	29.13	SK T-Brain	S. Hong, S. Kang, D. Cho [58]
Airia-GA-Cascade	25.99	Inst. of Automation, Chinese Acad. of Sci.	Y. Zhu, Q. Chen [61]
BetterFPN	28.55	ShanghaiTech Univ.	J. Hu, L. Jin [58]
Cascade R-CNN+	17.67	Fraunhofer IOSB	J. Meier, L. Sommer, L. Steinmann, A. Schumann [61]
Cascade CNN++	R-18.33	Univ. of Hong Kong	H. Han, J. Fan [61]
CenterNet	26.03	National Univ. of Singapore*, Pensees.ai <sup>†</sup> , Xidian Univ. <sup>‡</sup>	Y. Li*, Z. Wang <sup>†</sup> , Y. Toh <sup>†</sup> , F. Bai <sup>‡</sup> , J. Shen <sup>†</sup> [64]
CenterNet-Hourglass	22.36	Harbin Inst. of Tech.*, Inst. of Automation, Chinese Acad. of Sci. <sup>†</sup>	D. Yu*, L. Huang <sup>†</sup> , X. Zhao <sup>†</sup> , K. Huang <sup>†</sup> [64]
CNANet	26.35	Chongqing Univ.	Keyang Wang, Lei Zhang [61]
CN-DhVaSa	27.83	Siemens Tech. and Services Private Limited	D. Pailla, V. Kollerathu, S. Chennamsetty [64]
ConstraintNet	16.09	Xidian Univ.	D. Zeng, D. Li [64]
DA-RetinaNet	17.05	Nanjing Univ. of Posts and Telecom.	J. Xu, D. Cong [57]
DBCL	16.78	Snowcloud.ai	W. Dai, W. Wang [65]
DCRCNN	17.79	BTS Digital	A. Zinollayev, A. Askergaliyev [61]
DPNet-ensemble	<b>29.62</b>	Univ. of Elec. Sci. & Tech. of China	Q. Cheng, H. Qiu, Z. Song, H. Li [61]
DPN	25.09	Inst. of Auto., Chinese Acad. of Sci.	N. Xu, X. Zhang, B. Mao, C. Huo, C. Pan [61]
EHR-RetinaNet	26.46	Hanyang Univ.	J. Kim, B. Lee, C. Ma, J. Choi, S. Yang [57]
EnDet	17.81	Beijing Inst. of Tech.	P. Zhang, Y. Zhong [55], [60]
ERCNNs	20.45	Kakao Brain	J. Lee, I. Kim [55], [61]
FS-RetinaNet	26.31	Beijing Inst. of Tech.*, Samsung Stanford <sup>†</sup>	Z. Liu*, J. Ge*, T. Wu*, L. Sun <sup>†</sup> , G. Gao* [57]
GravityNet	25.66	Univ. of Glasgow	T. Heng, H. Nguyen [64]
HRDet+	28.39	South China Univ. of Tech.	J. Zhou, W. Qin, Q. Liu, H. Xiong [66]
HTC-drone	22.61	Queen Mary Univ. of London	X. Zhang [67]
Libra-HBR	25.57	Zhejiang Univ.	C. Deng, S. He, Q. Zeng, Z. Duan, B. Zhang [61], [68], [69]
MOD-RETINANET	16.96	Harman	A. Kumar, G. Jose, S. Kruthiventi [57]
MSCRDet	25.13	Dalian Univ. of Tech.	X. Chen, C. Liu, S. Chen, X. Zhang, D. Wang, H. Lu [61]
ODAC	17.42	Sun Yat-Sen Univ.	J. Zhang, J. Huang, X. Chen, D. Zhang [58]
retinaplus	20.57	Northwestern Poly. Univ.	Z. Zhang, P. Wang [57]
RRNet	29.13	Ocean Univ. of China	C. Chen, Y. Zhang, Q. Lv, X. Wang, S. Wei, X. Sun [64]
SAMFR-Cascade RCNN	20.18	Xidian Univ.	H. Wang, Z. Wang, M. Jia, A. Li, T. Feng [61]
S+D	28.59	Harbin Inst. of Tech.	Y. Chen [61], [66], [70]
SGE-Cascade CNN	R-27.33	Xi'an Jiaotong Univ.	X. Wei, Hao Qi, W. Li, G. Liu [61]
TridentNet	22.51	Huazhong Univ. of Sci. and Tech.	X. Zhang [71]
TSEN	23.83	Nanjing Univ. of Sci. and Tech.	Z. Zhu, Z. Li [55], [69], [72]

RCNN [59], RefineDet [62], DetNet [91], Cascade R-CNN [61], and CornerNet [84], shown in Table 3.

## 4.5 Results and Analysis

**Results on the test-challenge set.** Top 10 object detectors in the VisDrone-DET 2018 [27] and 2019 [28] challenges are presented in Table 3. In contrast to existing object detection datasets, *e.g.*, MS COCO [4], Caltech [1], and UA-

TABLE 3: Comparison results of the algorithms on the VisDrone-DET dataset.

Method	AP[%]	AP <sub>50</sub> [%]	AP <sub>75</sub> [%]	AR <sub>1</sub> [%]	AR <sub>10</sub> [%]	AR <sub>100</sub> [%]	AR <sub>500</sub> [%]
VisDrone-2018 challenge:							
HAL-Retina-Net	<b>31.88</b>	46.18	<b>32.12</b>	0.97	7.50	34.43	<b>90.63</b>
DPNet	30.92	<b>54.62</b>	31.17	1.05	8.00	<b>36.80</b>	50.48
DE-FPN	27.10	48.72	26.58	0.90	6.97	33.58	40.57
CFE-SSDv2	26.48	47.30	26.08	1.16	<b>8.76</b>	33.85	38.94
RD <sup>4</sup> MS	22.68	44.85	20.24	1.55	7.45	29.63	38.59
L-H RCNN+	21.34	40.28	20.42	1.08	7.81	28.56	35.41
Faster R-CNN2	21.34	40.18	20.31	<b>1.36</b>	7.47	28.86	37.97
RefineDet+	21.07	40.98	19.65	0.78	6.87	28.25	35.58
DDFPN	21.05	42.39	18.70	0.60	5.67	28.73	36.41
YOLOv3_DP	20.03	44.09	15.77	0.72	6.18	26.53	33.27
VisDrone-2019 challenge:							
DPNet-ensemble	<b>29.62</b>	<b>54.00</b>	<b>28.70</b>	0.58	3.69	17.10	42.37
RRNet	29.13	55.82	27.23	<b>1.02</b>	<b>8.50</b>	<b>35.19</b>	<b>46.05</b>
ACM-OD	29.13	54.07	27.38	0.32	1.48	9.46	44.53
S+D	28.59	50.97	28.29	0.50	3.38	15.95	42.72
BetterFPN	28.55	53.63	26.68	0.86	7.56	33.81	44.02
HRDet+	28.39	54.53	26.06	0.11	0.94	12.95	43.34
CN-DhVaSa	27.83	50.73	26.77	0.00	0.18	7.78	46.81
SGE-cascade R-CNN	27.33	49.56	26.55	0.48	3.19	11.01	45.23
EHR-RetinaNet	26.46	48.34	25.38	0.87	7.87	32.06	38.42
CNANet	26.35	47.98	25.45	0.94	7.69	32.98	42.28
VisDrone-dev:							
CornerNet [84]	<b>23.43</b>	<b>41.18</b>	<b>25.02</b>	<b>0.45</b>	<b>4.24</b>	<b>33.05</b>	<b>34.23</b>
Light-RCNN [59]	22.08	39.56	23.24	0.32	3.63	31.19	32.06
FPN [58]	22.06	39.57	22.50	0.29	3.50	30.64	31.61
Cascade R-CNN [61]	21.80	37.84	22.56	0.28	3.55	29.15	30.09
DetNet [91]	20.07	37.54	21.26	0.26	2.84	29.06	30.45
RefineDet [62]	19.89	37.27	20.18	0.24	2.76	28.82	29.41
RetinaNet [57]	18.94	31.67	20.25	0.14	0.68	7.31	27.59

DETRAC [8]), one of the most challenging issues in the VisDrone-DET dataset is the extremely small scale of objects.

As shown in Table 3, we find that HAL-Retina-Net and DPNet are the only two methods achieving more than 30% AP in the VisDrone-DET 2018 challenge. Specifically, HAL-Retina-Net uses the Squeeze-and-Excitation [87] and downsampling-upsampling [88] modules to learn both the channel and spatial attentions on multi-scale features. To detect small scale objects, it removes higher convolutional layers in the feature pyramid. The second best detector DPNet uses the Feature Pyramid Networks (FPN) [58] to extract multi-scale features and uses ensemble mechanism to combine three detectors with different backbones, *i.e.*, ResNet-50, ResNet-101 and ResNeXt. Similarly, DE-FPN and CFE-SSDv2 also employ multi-scale features, which rank in the third and fourth places with 27.10% and 26.48% AP scores, respectively. RD<sup>4</sup>MS trains 4 variants of RefineDet [62], *i.e.*, three use SEResNeXt-50 and one uses ResNet-50 as the backbone network. Moreover, DDFPN, ranked in the 9-th place, introduces deep back-projection super-resolution network [92] to upsample the image using the deformable FPN architecture [90]. Notably, most of the submitted methods use multi-scale testing strategy in evaluation, which is effective to improve performance.

In the VisDrone-DET 2019 challenge, DPNet-ensemble achieves the best results with 29.62% AP score. It uses the global context module [89] to integrate context information and deformable convolution [90] to enhance the transformation modeling capability of the detector. RRNet and ACM-OD tie for the second place in ranking with 29.13% AP score. RRNet is improved from [64] by integrating a re-regression module, formed by the ROIAlign module [81] and several convolution layers. ACM-OD introduces an active learning strategy, which is conducted with data augmentation for better performance.

In summary, as shown in Table 3, although the top detector DPNet-ensemble in the VisDrone-DET 2019 challenge is slightly inferior than the top detector HAL-Retina-Net in the VisDrone-DET 2018 challenge in terms of AP score, we can observe that the average AP score of the top 10 methods in

the VisDrone-DET 2019 challenge is greatly improved compared to that in the VisDrone-DET 2018 challenge. However, the top accuracy on this dataset is only 31.88%, achieved by HAL-Retina-Net in the VisDrone-DET 2018 challenge. It indicates the difficulty of the collected dataset and the badly need of developing more robust methods for real-world applications.

**Results on the test-dev set.** We present the evaluation results of the state-of-the-art methods in Table 3. CornerNet [84] achieves the top AP score 23.43, which uses the Hourglass-104 backbone for feature extraction. In contrast to FPN [58] and RetinaNet [62] with extra stages against the image classification task to handle objects with various scales, DetNet [91] re-designs the backbone network for object detection, which maintains the spatial resolution and enlarges the receptive field, achieving 20.07 AP score. Meanwhile, RefineDet [62] with the VGG-16 backbone performs better than RetinaNet [57] with the ResNet-101 backbone, *i.e.*, 19.89% *vs.* 18.94% in terms of AP score. This is because RefineDet [62] uses the object detection module to regress the locations and sizes of objects based on the coarsely adjusted anchors from the anchor refinement module.

## 4.6 Discussion

Captured by the cameras equipped on drones, the VisDrone-DET dataset is extremely challenging due to scale variation, occlusion, and class imbalance. Compared to traditional object detection datasets, there are more issues worth exploring in drone captured visual data.

**Annotation and evaluation protocol.** As shown in Fig. 4, there are groups of objects heavily occluded in drone captured visual data (see the orange bounding boxes of bicycles). If we use Non-maximum Suppression (NMS) to suppress duplicate detections in detectors, the majority of true positive objects will be inevitably removed. In some real applications, it is unnecessary and impractical to locate each individual object in the crowd. Thus, it is more reasonable to use a large bounding box with a count number to represent the group of objects in the same category (see the white bounding box of bicycle). Meanwhile, if we use the new annotation remedy, we need to redesign the metric to evaluate detection algorithms, *i.e.*, both the localization and counting accuracy should be considered in evaluation.

**Coarse segmentation.** Current object detection methods use bounding boxes to indicate object instances, *i.e.*, a 4-tuple  $(x, y, w, h)$ , where  $x$  and  $y$  are the coordinate of the bounding box's top-left corner, and  $w$  and  $h$  are the width and height of the bounding box. As shown in Fig. 4, it is difficult to predict the location and size of the pedestrian (see the yellow bounding box) due to occlusion and non-rigid deformation of human body. A possible way to mitigate such issue is to integrate coarse segmentation into object detection, which might be effective to remove the disturbance of background area enclosed in the bounding box of non-rigid objects, such as *person* and *bicycle*, see Fig. 4. In summary, this interesting problem is still far from being solved and worth to explore.

## 5 VID TRACK

The VID track aims to locate object instances from a pre-defined set of categories in the video sequences. That is,

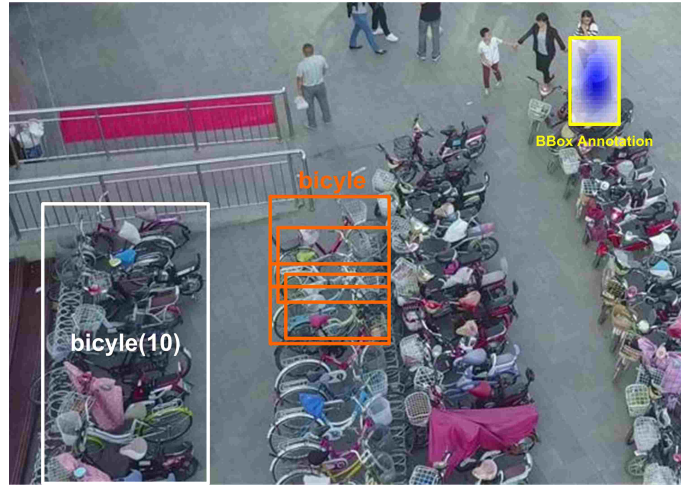


Fig. 4: Descriptions of the challenging issues in the image object detection task.

given a series of video clips, the algorithms are required to produce a set of bounding boxes of each object instance in each video frame (if any), with real-valued confidences. In contrast to DET track focusing on object detection in individual images, we deal with detection object instances in video clips, which contain temporal consistency in consecutive frames. Five categories of objects are considered in this track, *i.e.*, *pedestrian*, *car*, *van*, *bus*, and *truck*. Similar to the DET track, some rarely occurring special vehicles (*e.g.*, *machineshop truck*, *forklift truck*, and *tanker*) are ignored in evaluation. The AP score across different object categories and IoU thresholds of algorithm predictions in individual frames are used to evaluate the quality of the results.

### 5.1 Data Collection and Annotation

We provide 96 challenging video clips in the VID track, including 56 clips for training (24,198 frames in total), 7 for validation (2,846 frames in total), 16 for testing (6,322 frames in total) and 17 for testing (6,635 frames in total). To clearly describe the data distribution, we plot the number of objects per frame *vs.* percentage of frames in Fig. 5, and the number of objects of different object categories in Fig. 6. As shown in Fig. 5, the class imbalance issue is extremely severe in the VID and MOT datasets, challenging the performance of algorithms. For example, in the training set, the number of *car* trajectories is more than  $50\times$  of the number of *car* trajectories. Meanwhile, as shown in Fig. 5, the length of object trajectories varies dramatically, *e.g.*, the maximal and minimal lengths of object trajectories are 1 and 1,255, requiring the tracking algorithms to perform well in both short-term and long-term cases.

We manually annotate five categories of objects in each video clip, *i.e.*, *pedestrian*, *car*, *van*, *bus*, and *truck*, and conduct the cross-checking to ensure the annotation quality. Similar to the DET track, we also provide the annotations of occlusion and truncation ratios of each object and ignored regions in each video frame. We present the annotation exemplars in the second row of Fig. 1.

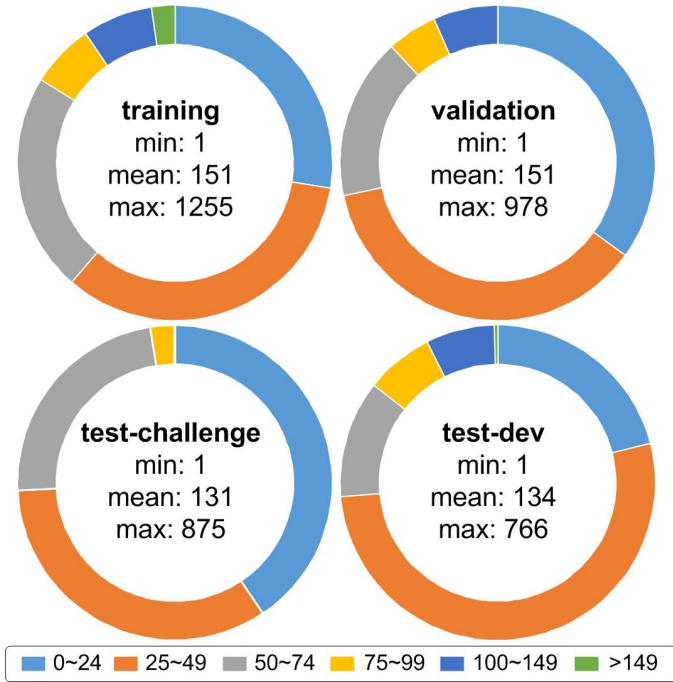


Fig. 5: The length of object trajectories *vs.* the percentage of trajectories in the training, validation, test-challenge and test-dev subsets of the *VID* and *MOT* tracks.

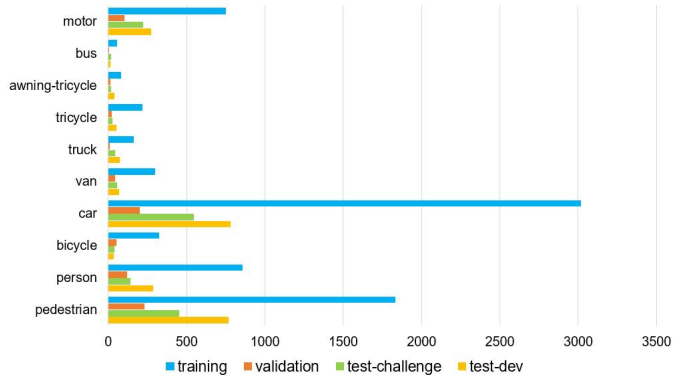


Fig. 6: The number of object trajectories in different categories in the training, validation, test-challenge and test-dev subsets of the *VID* and *MOT* tracks.

## 5.2 Evaluation Protocol

For the *VID* track, each algorithm is required to generate a list of bounding boxes with confidence scores in each video frame. Following the evaluation protocol in MS COCO [4] and ILSVRC [93], we use the  $AP^{IoU=0.50:0.05:0.95}$ ,  $AP^{IoU=0.50}$ ,  $AP^{IoU=0.75}$ ,  $AR^{max=1}$ ,  $AR^{max=10}$ ,  $AR^{max=100}$  and  $AR^{max=500}$  scores to evaluate the video object detection algorithms. Notably, the  $AP^{IoU=0.50:0.05:0.95}$  score is used as the primary metric. Please refer to [4], [93] for more details.

## 5.3 Brief Review of VID Algorithms

The researchers generally extend image object detection methods to solve video object detection by exploiting temporal coherence of objects to handle appearance deterior-

TABLE 4: Teams participating in VisDrone-VID 2018 and 2019 challenges, ordered alphabetically.

Codename	AP	Institutions	Contributions and References
VisDrone-2018 Challenge:			
CERTH-ODV	9.10	Centre for Res. & Tech. Hellas	E. Michail, K. Avgerinakis, P. Giannakeris, S. Vrochidis, I. Kompatsiaris [55]
CFE-SSDv2	21.57	Peking Univ.	Q. Zhao, F. Ni, Y. Wang [56]
EODST	16.54	Xidian Univ.	Z. Pi, Y. Wu, M. Liu [56], [94]
FGFA+	16.00	Xidian Univ.	J. Gao, Y. Bai, G. Zhang, D. Wang, Q. Ma [95]
RD	14.95	Fraunhofer IOSB*, Karlsruhe Inst. of Tech.†	O. Acatay*, L. Sommer*†, A. Schumann* [62]
RetinaNet_s	8.63	Beijing Univ. of Posts and Telecom.	J. Zhao, Y. Zhao [57]
VisDrone-2019 Challenge:			
AFSRNet	24.77	Beijing Inst. of Tech.*, Samsung Inc†	Z. Liu*, J. Ge*, T. Wu*, L. Sun†, G. Gao* [57], [86]
CN-DhVaSa	21.58	Siemens	D. Pailla, V. Kollerathu, S. Chennamsetty [64]
CornerNet-lite-FS	12.65	Ocean Univ. of China	X. Sun, H. Xu, M. Zhang, Z. Dong, L. Du [96]
DBAI-Det	29.22	DeepBlue Tech.	Z. Luo, F. Ni, B. Dong, Y. Yao, Z. Xu [61]
DetKITSY	20.43	Karlsruhe Inst. of Tech.*, Sun Yat-sen Univ.†, VIPioneers (Huituo) Inc†	W. Tian*, J. Hu†, Y. Song*, Z. Chen†, L. Chen†, M. Lauer* [61]
DM2Det	13.52	KARI*, KAIST†	S. Moon*, D. Lee*, Y. Kim*, S. Moon† [97]
EODST++	18.73	Xidian Univ.	Zhaoliang Pi, Yingping Li, X. Chen, Y. Lian, Y. Wu [56], [85], [98], [99]
FT	9.15	Northwestern Poly. Univ.	Y. Zhang, Y. Wang, Y. Li [55]
FRCFPN	16.50	Nanjing Univ. of Sci. & Tech.	Z. Zhu, Z. Li [55], [100]
HRDet+	23.03	South China Univ. of Tech.	J. Zhu, W. Qin, Q. Liu, H. Xiong [66]
Libra-HBR	18.29	Zhejiang Univ.	C. Deng, Q. Zeng, Z. Duan, B. Zhang [61], [68], [69]
Sniper+	18.16	Xi'an Jiaotong Univ.	X. Zhao, T. Sun, G. Liu [68]
VCL-CRCNN	21.61	Tsinghua Univ.	Z. Xiao [61]

ation such as motion blur, video defocus, *etc.* Some algorithms aggregate object features in several video frames for video object detection, including HOG [101], DFF [102], FGFA [95], STMM [103]. Associate object detections in consecutive video frames is another effective way to construct a robust tracker, such as Seq-NMS [104], D&T [105], T-CNN [106]. Long time partially or fully occlusion, severe camera view changes, and fast motion are new challenging factors for video object detection methods in the proposed drone-captured video sequences.

## 5.4 Submitted Algorithms

**VisDrone 2018 challenge.** We have received 6 entries in the *VID* track of the VisDrone-2018 challenge [31], shown in Table 4. Four methods are directly derived from image object detectors, *i.e.*, CERTH-ODV, CFE-SSDv2, RetinaNet\_s, and RD. The EODST method is constructed based on SSD [56], and uses the ECO tracker [94] to exploit the temporal coherence. FGFA+ is modified from the video object detection framework [95] by enhancing contrast and brightness of frames. CFE-SSDv2 achieves the top accuracy (*i.e.*, 21.57 AP), which uses a comprehensive feature enhancement module to enhance the features for small objects.

**VisDrone 2019 challenge.** As presented in Table 4, 13 video detection methods are submitted in this track [32]. Similar to VisDrone-VID2018 challenge, the majority of submissions are directly derived from object detectors on static images. For instance, there are 3 methods based on Cascade R-CNN [61], *i.e.*, DBAI-Det, DetKITSY and VCL-CRCNN. Libra-HBR combines improved SNIPER [68], Libra R-CNN [69] and cascade R-CNN [61]. CN-DhVaSa and CornerNet-lite-FS are based on the anchor-free methods CenterNet [64] and CornerNet [96], respectively. AFSRNet integrates feature selected anchor-free head (FSAF) [86] into RetinaNet [57] to improve the accuracy. FRCFPN is derived from Faster R-CNN [55] with data augmentation [100]. EODST++ improves the method EODST in VisDrone-VID 2018 challenge, using SSD [56] and FCOS [85] for detection in individual frames, and ECO [98] and SiamRPN++ [99] to track objects to recall false negatives in detection. FT improves Faster R-

TABLE 5: Comparison results of the algorithms on the VisDrone-VID dataset.

Method	AP[%]	AP <sub>50</sub> [%]	AP <sub>75</sub> [%]	AR <sub>1</sub> [%]	AR <sub>10</sub> [%]	AR <sub>100</sub> [%]	AR <sub>500</sub> [%]
VisDrone-2018 challenge:							
CFE-SSDv2	21.57	44.75	17.95	11.85	30.46	41.89	44.82
EODST	16.54	38.06	12.03	10.37	22.02	25.52	25.53
FGFA+	16.00	34.82	12.65	9.63	19.54	22.37	22.37
RD	14.95	35.25	10.11	9.67	24.60	29.72	29.91
CERTH-ODV	9.10	20.35	7.12	7.02	13.51	14.36	14.36
RetinaNet <sub>s</sub>	8.63	21.83	4.98	5.80	12.91	15.15	15.15
VisDrone-2019 challenge:							
DBAI-Det	29.22	58.00	25.34	14.30	35.58	50.75	53.67
AFSRNet	24.77	52.52	19.38	12.33	33.14	45.14	45.69
HRDet+	23.03	51.79	16.83	4.75	20.49	38.99	40.37
VCL-CRCNN	21.61	43.88	18.32	10.42	25.94	33.45	33.45
CN-DhVaSa	21.58	48.09	16.76	12.04	29.60	39.63	40.42
DetKITSY	20.43	46.33	14.82	8.64	25.80	33.40	33.40
ACM-OD	18.82	43.15	13.42	5.98	22.29	34.78	35.92
EODST++	18.73	44.38	12.68	9.67	22.84	27.62	27.62
Libra-HBR	18.29	44.92	11.64	10.69	26.68	35.83	36.57
Sniper+	18.16	38.56	14.79	9.98	27.18	38.21	39.08
VisDrone-dev:							
FGFA [95]	14.44	33.34	11.85	7.29	21.37	27.09	27.21
D&T [105]	14.21	32.28	10.39	7.59	19.39	26.57	25.64
FPN [58]	12.93	29.88	10.12	7.03	19.71	25.59	25.99
CenterNet [64]	12.35	28.93	9.92	6.41	18.93	24.87	24.87
CornerNet [84]	12.29	28.37	9.48	6.07	18.60	24.03	24.03
Faster-RCNN [55]	10.25	26.83	6.70	5.93	12.98	13.55	13.55

CNN [55] based on three-dimensional convolution to exploit temporal information for better performance.

**VisDrone-dev benchmark.** We evaluate 2 state-of-the-art video object detection methods, *i.e.*, FGFA [95] and D&T [105], and 4 state-of-the-art image object detection methods, *i.e.*, Faster R-CNN [55], FPN [58], CornerNet [84], and CenterNet [64], in this track. Specifically, FPN [58] and Faster R-CNN [55] are anchor-based methods, and CornerNet [84] and CenterNet [64] are anchor-free methods. The FGFA [95] and D&T [105] methods attempt to exploit temporal coherence of objects in consecutive frames to improve the performance.

## 5.5 Results and Analysis

**Results on the test-challenge set.** We report the evaluation results of the submissions in the VisDrone-VID 2018 [31] and 2019 [32] challenges in Table 5. CFE-SSDv2 obtains the best AP score 21.57% in the VisDrone-VID 2018 challenge, which is improved from SSD [56] by integrating a comprehensive feature enhancement module for accurate results, especially for small objects. Different from CFE-SSDv2, EODST exploits temporal information to associate object detections in individual frames using the ECO tracking algorithm [94], achieving the second best AP 16.54%. FGFA+ ranks in the third place with 16.00% AP, which is a variant of video object detection method FGFA [95] with various data augmentation strategies.

In the VisDrone-VID 2019 challenge, researchers propose more powerful algorithms, which benefit from several state-of-the-art detectors, such as HRDet [66], Cascade R-CNN [61], CenterNet [64], RetinaNet [57], FPN [58]. All top 5 detectors, *i.e.*, DBAI-Det, AFSRNet, HRDet+, VCL-CRCNN and CN-DhVaSa, surpass the top detector CFE-SSDv2 in the VisDrone-VID 2018 challenge. We witness the significant improvement of the performance of video object detection methods. However, there still remains much room for improvement. DBAI-Det achieves the best results with 29.22% AP, which is constructed based on Cascade R-CNN [61] with ResNeXt101 [107], and integrates the deformable convolution operation [90] and global context module [89] to improve the performance. AFSRNet ranks the second place with 24.77% AP, which integrates the feature selected

anchor-free head [86] into RetinaNet [57]. HRDet+, VCL-CRCNN and CN-DhVaSa rank in the third, forth, and fifth places, which are improved from HRDet [66], Cascade R-CNN [61], and CenterNet [64], respectively. To deal with large scale variations of objects, other top detectors, such as DetKITSY and EODST++, employ multi-scale features and proposals for detection, which performs better than the state-of-the-art video object detector FGFA [95]. Notably, most of the video object detection methods are computationally expensive for practical applications, whose running speed are less than 10 fps on a workstation with GTX 1080Ti GPU.

**Results on the test-dev set.** The evaluation results of 2 state-of-the-art video object detection methods [95], [105], and 4 state-of-the-art image object detection methods [55], [58], [64], [84] on the test-dev set are presented in Table 5. We find that the two video object detectors performs much better than the four image object detectors. For example, the second best video object detector D&T [105] improves 1.28% in AP score compared to the top image object detector FPN [58], which demonstrates the importance of exploiting the temporal information in video object detection. FGFA [95] leverages temporal coherence to enhance the features of objects for accurate results. D&T [105] simultaneously solves detection and tracking with an end-to-end trained convolutional neural network, and a multi-task loss for frame-based object detection and across-frame track regression. However, how to exploit temporal information is still an open question for video object detection.

## 5.6 Discussion

Different from the DET task, the accuracy of detection methods suffers from degenerated object appearances in videos such as motion blur, pose variations, and video defocus. Exploiting temporal coherence and aggregating features in consecutive frames might to be two effective ways to handle such issue.

**Temporal coherence.** A feasible way to exploit temporal coherence is using object trackers, *e.g.*, ECO [98] and SiamRPN++ [99], into detection algorithms. Specifically, we can assign a tracker to each detected object instance in individual frames to guide detection in consecutive frames, which is effective to suppress false negatives in detection. Meanwhile, integrating re-identification module is another promising way to exploit temporal coherence for better performance, just as described in D&T [105].

**Feature aggregation.** Aggregating features in consecutive frames is also a useful way to improve the performance. As stated in FGFA [95], aggregating nearby features along the motion paths to leverage temporal coherence significantly improves the detection accuracy. Thus, we can take several consecutive frames as input, and feed them into deep neural networks to extract temporal salient features using 3D convolution operations or optical flow algorithm.

## 6 SOT TRACK

For the SOT track, we focus on generic single object tracking, also known as model-free tracking [5], [108], [109]. In particular, for an input video sequence and the initial bounding

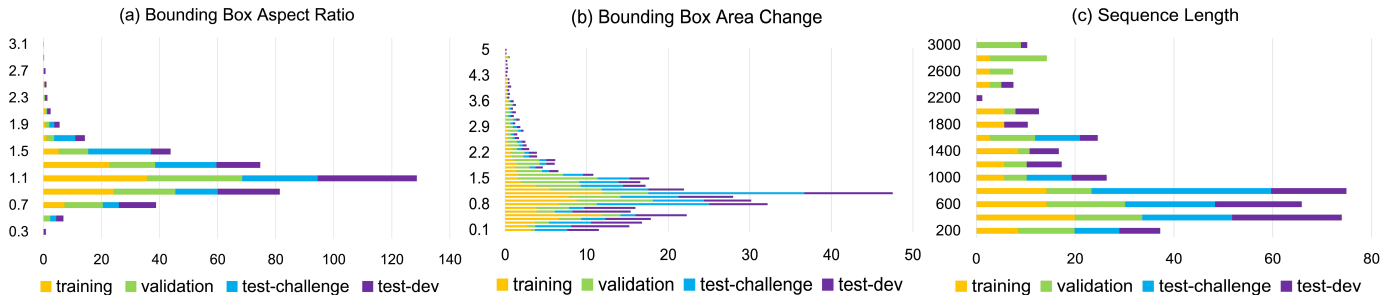


Fig. 7: (a) The number of frames *vs.* the aspect ratio (height divided by width) change rate with respect to the first frame, (b) the number of frames *vs.* the area variation rate with respect to the first frame, and (c) the distributions of the number of frames of video clips, in the `training`, `validation`, `test-challenge` and `test-dev` subsets for the *SOT track*.

box of the target object in the first frame, the *SOT track* requires the algorithms to locate the target bounding boxes in the subsequent video frames. The tracking targets in these sequences include *pedestrians*, *cars*, *buses*, and *animals*.

### 6.1 Data Collection and Annotation

In 2018, we provide 167 video sequences with 139,276 fully annotated frames, split into four subsets, *i.e.*, the `training` set (86 sequences with 69,941 frames in total), `validation` set (11 sequences with 7,046 frames in total), `testing-challenge 2018` set (35 sequences with 29,367 frames in total), and `testing-dev` set (35 sequences with 32,922 frames in total). Notably, the `testing-challenge 2018` subset is designed to evaluate the algorithms submitted in the VisDrone-SOT 2018 challenge competition. To thoroughly evaluate the performance of algorithms in long-term tracking, we add 25 new collected sequences with 82,644 frames in total in the `test-challenge 2018` set to form the `test-challenge 2019` set, which is used in the VisDrone-SOT 2019 challenge competition. The tracking targets in all these sequences include *pedestrian*, *cars*, and *animals*. The statistics of target objects, *i.e.*, the aspect ratio in different frames, the area change ratio, and the sequence length are presented in Fig. 7.

The enclosing bounding box of target object in each video frame is annotated to evaluate the performance of trackers. To thoroughly analyze the tracking performance, we also annotate 12 sequence attributes following [10], *i.e.*, *aspect ratio change*, *background clutter*, *camera motion*, *fast motion*, *full occlusion*, *illumination variation*, *low resolution*, *out-of-view*, *partial occlusion*, *scale variation*, *similar object*, and *viewpoint change*. Please refer to [10] for more details.

### 6.2 Evaluation Protocol

According to [5], we use the success and precision scores to evaluate trackers. Specifically, we plot the success curve, *i.e.*, the percentage of successfully tracked frames *vs.* bounding box overlap threshold in the range  $[0, 1]$ . The success score is computed based on the area under the success plot, which is the primary metric for ranking trackers. The successfully tracked frames are determined by the overlap  $O$  between the predicted bounding box  $\hat{\alpha}$  and the ground-truth bounding box  $\alpha^*$ . If the overlap  $O$  is larger than a threshold, we regard it as successfully tracked frame, and vice versa. The overlap  $O = \frac{|\hat{\alpha} \cap \alpha^*|}{|\hat{\alpha} \cup \alpha^*|}$ , where  $\cap$  and  $\cup$  are the

intersection and union between the two regions respectively, and  $|\cdot|$  denote the number of pixels within the region. The precision score denotes the percentage of frames such that the Euclidean distance between predicted locations and ground-truth locations are within 20 pixels in the image plane. Please refer to [5] for more details.

### 6.3 Brief Review of SOT Algorithms

SOT is a hot topic in the last decade. Early visual tracking methods rely on extracting hand-crafted features of candidate target regions, and use matching algorithms [126], [127] or hand-crafted discriminative classifiers [128], [129] to generate tracking results. Several tracking algorithms attempt different kinds of appearance representation strategies of objects, such as pixel-based model [130], [131], [132], part-based model [133], [134], [135] and holistic model [136], [137], [138]. The aforementioned appearance representation methods can be integrated into the correlation filter framework [116], [139], [140], [141], [142] to achieve accurate tracking results.

In recent years, the pre-trained deep convolutional neural network (CNN) are applied to extract features for SOT [98], [143]. Some methods [111], [144] design different network architectures to improve the performance. Siamese network (*e.g.*, SiamRPN++ [99], SiamMask [145] and SiamMan [109]) is one of the most popular network in SOT with attractive performance, which optimize the similarities between the regions of target object and the candidate regions. The LSTM network is also explored to capture the historical context information for visual tracking, such as MAM [146] and FPRNet [147]. Although significant progress has been made in visual tracking field, it is still difficult for the state-of-the-art trackers to produce accurate results on the drone-captured video sequences, due to several challenging factors such as abrupt camera motion and small scales of targets.

### 6.4 Submitted Algorithms

**VisDrone 2018 challenge.** We present the results and team information in this track [29] in Table 6, including 17 entries from 26 different institutes. CFWCRKF, CKCF, DCST and STAPLE\_SRCR are based on the correlation filters, while C3DT, VITALD, DeCom and BTT are improved from the deep MDNet method [111]. Seven other trackers combine the CNN models and correlation filter algorithms, *i.e.*,

TABLE 6: Teams participating in VisDrone-SOT 2018 and 2019 challenges, ordered alphabetically.

CodeName	Success Score	Institutions	Contributors and References
VisDrone-2018 Challenge:			
AST	56.2	Beihang Univ.* <sup>†</sup> , Lancaster Univ. <sup>†</sup> , Shenyang Aerospace Univ. <sup>†</sup>	C. Liu*, W. Ding*, J. Yang*, B. Zhang* <sup>†</sup> , J. Han <sup>†</sup> , H. Chen <sup>†</sup> [110]
BTT	60.5	Shandong Univ.	K. Song, X. Hu, W. Wang, Y. Li, W. Zhang [111]
C3DT	53.6	South China Univ. of Tech.	H. Li, S. Wu [111]
CFCNN	55.2	Karlsruhe Inst. of Tech.	W. Tian, M. Lauer [112]
CFWCRKF	50.6	Beijing Univ. of Posts and Telecom.	S. Zhu, Y. Zhao [113]
CKCF	32.3	Centre for Res. & Tech. Hellas	E. Michail, K. Avgerinakis, P. Giannakeris, Stefanos Vrochidis, I. Kompatsiaris [114]
DCFNet	47.4	Civil Aviation Univ. of China*, Inst. of Auto, Chinese Acad. of Sci. <sup>†</sup>	J. Li*, Q. Wang <sup>†</sup> , W. Hu <sup>†</sup> [115]
DCST	52.8	Nanjing Artificial Intell. Chip Res., IACAS* <sup>†</sup> , Inst. of Auto., Chinese Acad. of Sci. <sup>†</sup> , Nanjing Univ. of Info. Sci. & Tech. <sup>†</sup>	J. Fan*, Y. Zhang* <sup>†</sup> , J. Cheng* <sup>†</sup> , K. Zhang <sup>†</sup> , Q. Liu <sup>†</sup> [116]
DeCoM	56.9	Seoul National Univ.* <sup>†</sup> , NAVER Corp <sup>†</sup>	B. Heo*, S. Yun <sup>†</sup> , J. Choi* [111]
IMT3	17.6	Univ. of South Australia	A. Perera
LZZ-ECO	68.0	Xidian Univ.	X. Li, J. Zhang, X. Zhang [94]
OST	50.3	Univ. of Ottawa	Y. Wang, L. Ding, R. Laganière, X. Luo [94]
TRACA+	45.7	Seoul National Univ.* <sup>†</sup> , Samsung R&D Campus <sup>†</sup>	K. Lee*, J. Choi* <sup>†</sup> , J. Choi* [117]
SDRCO	56.3	Beijing Univ. of Posts and Telecom.* <sup>†</sup> , Tencent <sup>†</sup> , Sun yat-sen Univ. <sup>†</sup> , Tsinghua Univ. <sup>†</sup>	Z. He*, R. Zhang <sup>†</sup> , P. Zhang <sup>†</sup> , X. He <sup>†</sup> [113]
SECFNet	51.1	National Univ. of Defense Tech.* <sup>†</sup> , Shanghai Jiao Tong Univ. <sup>†</sup>	D. Li*, Y. Kuai*, H. Liu*, Z. Deng*, J. Zhao <sup>†</sup> [118]
STAPLE_SRCA	61.9	Xidian Univ.	W. Zhang, Y. Meng [119]
VITALD	62.8	Harbin Inst. of Tech.* <sup>†</sup> , Univ. of Chinese Acad. of Sci. <sup>†</sup> , Inst. of Computing Tech., Chinese Acad. of Sci. <sup>†</sup>	Y. Qi*, Y. Yang <sup>†</sup> , W. Chen <sup>†</sup> , K. Duan <sup>†</sup> , Q. Xu <sup>†</sup> , Q. Huang* <sup>†</sup> [111], [120]
VisDrone-2019 Challenge:			
ACNT	53.2	Jiangnan Univ.* <sup>†</sup> , Univ. of Surrey <sup>†</sup>	T. Xu* <sup>†</sup> , X. Wu*, Z. Feng <sup>†</sup> , J. Kittler <sup>†</sup> [121]
AST	51.9	Nanjing Univ. of Info. Sci. & Tech.	K. Yang, X. Wang, N. Wang, J. Fan, K. Zhang [121]
ATOMFR	61.7	Xidian Univ.	W. Zhang, H. Wang, J. Zhou [121]
ATOMv2	46.8	Inst. of Auto., Chinese Acad. of Sci.	L. Huang, X. Zhao, K. Huang [121]
DATOM_AC	54.1	Northwestern Poly. Univ.	X. Xue, X. Yin, S. Zou, Y. Li [121]
DC-Siam	46.3	Northwestern Poly. Univ.	J. Zhou, P. Wang [99], [121], [122]
DR-V-LT	57.9	Tech. & Engr. Center for Space Utilization, Chinese Acad. of Sci.* <sup>†</sup> , Univ. of Chinese Acad. of Sci. <sup>†</sup>	S. Xuan* <sup>†</sup> , S. Li* <sup>†</sup> [99]
ED-ATOM	63.5	Inst. of Info. Engr., CAS*, Univ. of Chinese Acad. of Sci. <sup>†</sup> , CloudWalk Tech. <sup>3</sup>	C. Zhang* <sup>†</sup> , S. Zhao* <sup>†</sup> , K. Zhang* <sup>†</sup> , S. Li* <sup>†</sup> , H. Wen <sup>†</sup> , S. Ge* <sup>†</sup> [121]
MDNet_RPN	52.6	Xi'an Jiaotong Univ.	H. Wu, X. Yang, Y. Yang, G. Liu [111]
HCF	36.1	Yuneeq Aviation Tech.* <sup>†</sup> , Univ. of Ottawa <sup>†</sup> , Inst. of Info. Engr., Chinese Acad. of Sci. <sup>†</sup>	Z. Sun*, Y. Wang <sup>†</sup> , C. Zhang <sup>†</sup> [112]
MATOM	40.9	Inst. of Optics and Elec., CAS.	L. Zhou, Q. Hu [121]
PTF	54.4	Xidian Univ.	R. Zhang, J. Chen, J. Gao, X. Li, L. Shi [121]
SE-RPN	41.9	Wuhan Univ.	X. Lei, J. Wang [122]
SiamDW-FC	38.3	Inst. of Automation, CAS.	Z. Zhang, W. Hu [123]
SiamFCOT	47.2	Zhejiang Univ.	Y. Xu, Z. Wang [122]
Siam-OM	59.3	Xidian Univ.	X. Zhang, X. Li, J. Zhang [121], [124]
SiamRPN++	56.8	Zhejiang Univ.	Z. Duan, W. Zhu, X. Yu, B. Han, Z. Yu, T. He [99]
SMILE	59.4	Xidian Univ.	R. Ma, Y. Gao, Y. Yang, W. Song, Y. Li [99], [121]
SSRR	44.7	Nanjing Univ. of Info. Sci. & Tech.	N. Wang, K. Zhang [121]
Stable-DL	38.2	Univ. of Ottawa*, Shanghai Jiao Tong Univ. <sup>†</sup> , Beihang Univ. <sup>†</sup> , INSKY Lab, Leotail Intell. Tech <sup>†</sup>	Y. Wang*, L. Ding <sup>†</sup> , R. Laganière*, J. Wan <sup>†</sup> , Wei Shi <sup>†</sup>
TDE	37.2	Inst. of Info. Engr., CAS.* <sup>†</sup> , UCAS. <sup>†</sup> , Yuneeq Aviation Tech. <sup>†</sup> , Univ. of Ottawa <sup>†</sup>	C. Zhang* <sup>†</sup> , S. Zhao* <sup>†</sup> , Z. Sun <sup>†</sup> , Y. Wang <sup>†</sup> , S. Ge* [125]
TIOM	55.3	Beijing Univ. of Posts & Telecom.	S. Zhu, Y. Zhao [121]

CFCNN, DCFNet, LZZ-ECO, OST, TRACA+, SDRCO and SECFNet. Notably, OST, CFCNN and LZZ-ECO use object detectors to perform target re-detection for more robustness. AST predicts the target using saliency map and IMT3 is based on the normalized cross correlation filter. The LZZ-ECO method produces the best results with 68.0 success score, which uses YOLOv3 [60] to re-detect the drifted target and ECO [94] to track the target object.

**VisDrone 2019 challenge.** As shown in Table 6, there are 22 trackers from 19 different institutes submitted in this track [30]. Among them, 9 trackers are constructed based on ATOM [121], *i.e.*, ACNT, AST, ATOMFR, ATOMv2, DATOM\_AC, ED-ATOM, MATOM, SSRR and TIOM. Notably, ED-ATOM achieves the best performance with 63.5 success score and 90.0 precision score. PTF follows the ECO algorithm [98], and Siam-OM and SMILE use the Siamese networks based on ATOM [121]. 5 other trackers are also using the Siamese network architecture, including DC-Siam, DR-V-LT, SiamDW-FC, SiamFCOT and SiamRPN++.

**VisDrone-dev benchmark.** 21 state-of-the-art single-object tracking methods are evaluated for comparison in this track. We roughly divide them into three categories, *i.e.*, the correlation filters based, the siamese network based, and the convolutional network based approaches, listed as follows.

- *Correlation filters based approach:* KCF [114], CSRDCF [148], LCT [149], DSST [150], ECO [98], SRDCF [151], SCT [152], fDSST [153], Staple [116], Staple\_CA [119], BACF [112], PTAV [154], STRCF [110], and HCFT [155]<sup>8</sup>.
- *Siamese network based approach:* DSiam [156], SiameseFC [157], and SiamRPN++ [99].
- *Convolutional network based approach:* HCFT [155], MD-Net [111], CFNet [118], TRACA [158], and ATOM [121].

## 6.5 Results and Analysis

**Results on the test-challenge set.** The overall success and precision scores of top 10 submissions in the VisDrone-SOT 2018 [29] and 2019 [30] challenges are shown in Fig. 8(a) and (b), respectively. Notably, several challenging factors in the collected dataset, such as background clutter, large scale variation, and occlusion, make the trackers easily to drift. To that end, some trackers integrate the state-of-the-art detectors to re-detect the target when drifting occurs. For example, in the VisDrone-SOT 2018 challenge, LZZ-ECO combines YOLOv3 [60] and ECO [94] to achieve the best success score 68.0 and precision score 92.9. VITALD trains RefineDet [62] as a reference for the VITAL tracker [120], which obtains the second best success score 62.8 and the third best precision score 82.0. Another solution to deal with drifting problem is STAPLE\_SRCA [119], which develops a sparse context-aware response scheme to recognize whether the target moves out of the scene or be covered by other objects. It obtains the third best success score 61.9 and the second best precision score 87.1. DCST learns the spatio-temporal regularized correlation filters using color clustering based histogram model without the re-detection module, resulting in inferior results with 52.8 success score and 66.8 precision score.

We notice that the correlation filter based methods do not perform well in the VisDrone-SOT 2018 challenge. Thus, in the VisDrone-SOT 2019 challenge, the researchers shift their focus from correlation filter based methods to deep neural network based methods, such as ATOM [121] and Siamese networks [99], [156], [157]. Specifically, ATOMFR combines SENet [87] and ATOM [121] to capture the inter-dependencies within feature channels and suppress feature channels that are of little use to the current target size and location estimation, achieving the top accuracy on the test-challenge 2018 set with success score 75.5 and precision score 94.7.

Another critical engine for the performance improvements is the creation and utilization of large-scale datasets (*e.g.*, MS COCO [4], Got-10k [159], ImageNet DET/VID [3], LaSOT [9], TrackingNet [160], VOT [44] and YoutubeBB [161]) for deep neural network training. For example, ED-ATOM achieves the best results (*i.e.*, 63.5 success score and 90.0 precision score) in the VisDrone-SOT 2019 challenge.

8. Since HCFT [155] adaptively learns correlation filters on each convolutional layer to encode the target appearance, we category it into both the correlation filter and convolutional network based approaches.

This is because ED-ATOM is constructed based on ATOM [121] with the low-light image enhancement algorithm [162] and the online data augmentation scheme [163], [164]. Meanwhile, the model is trained on ImageNet DET/VID [3], MS COCO [4], Got-10k [159], and LaSOT [9].

Moreover, tracker combination is an effective strategy to improve the performance. Siam-OM uses ATOM [121] to handle short-term tracking, while DaSiam [124] with ResNet to handle long-term tracking, ranked in the fourth place in the VisDrone-SOT 2019 challenge. SIMLE combines two state-of-the-art trackers ATOM [121] and SiamRPN++ [99] to improve the performance, ranked in the fifth place. DR-V-LT integrates the distractor-aware verification network into SiamRPN++ [99], which is robust to similar objects challenge, ranked in the eighth place.

In addition, comparing the results of the submitted trackers on the `test-challenge 2018` and `test-challenge 2019` sets, we find that the tracking accuracy is significantly degraded. The best tracker ED-ATOM achieves success score 73.90 and precision score 95.80 on the `test-challenge 2018` set *vs.* success score 63.50 and precision score 90.00 on the `test-challenge 2019` set. It demonstrates the difficulties of the 25 new collected long-term tracking sequences, and suggests the need to develop more effective trackers for challenging scenarios on drones.

**Results on the `test-dev` set.** We evaluate 21 state-of-the-art trackers on the `test-dev` set in Fig. 8(c). As shown in Fig. 8(c), ATOM [121] (marked as the orange cross in the top-right corner) obtains the best 64.5 success score and the third best 83.0 precision score. This is attributed to the network trained offline on large-scale datasets to directly predict the IoU overlap between the target and a bounding box estimate. However, it performs not well in terms of *low resolution* and *out of view*. MDNet [111] and SiamRPN++ [99] rank the second and third places in terms of success score, respectively. In summary, training on large-scale datasets brings significant performance improvement of trackers.

## 6.6 Discussion

The state-of-the-art SOT algorithms on the VisDrone-SOT dataset are inspired by the algorithms in the object detection and re-identification fields. They benefit a lot from offline training on large-scale datasets, such as MS COCO [4], Got-10k [159], ImageNet DET/VID [3], LaSOT [9], TrackingNet [160], VOT [44] and YoutubeBB [161]. However, fast motion, low resolution, and occlusion still challenge the performance of the SOT algorithms.

**Abrupt motion.** Several SOT algorithms [99], [145], [165] formulate object tracking as the one-shot detection task, which use the bounding box in the first frame as the only exemplar. These methods rely on the pre-set anchor boxes to regress the bounding box of target in consecutive frames. However, the pre-defined anchor boxes can not adapt to various motion patterns and scales of targets, especially when the *fast motion* and *occlusion* occur. To this end, we can attempt to integrate the motion information or re-detection module to improve the accuracy of tracking algorithms.

**Low resolution** is another challenging factor greatly affects tracking accuracy. Most of the state-of-the-art methods [99], [121], [156] merely focus on the appearance variations of

target region, producing unstable and inaccurate results. We believe that exploiting context information surrounding the target and super-resolution technique can be helpful to improve the tracking performance.

**Occlusion** happens frequently in tracking process, which is the obstacle to the accurate tracking results. Some previous algorithms [46], [133], [135], [166] attempt to use part-based representations to handle the appearance changes caused by occlusion. Meanwhile, using re-initialization module [167] is an effective strategy to get rid of occlusion, *i.e.*, the re-initialization module is able to re-detect the target after reappearing in the scenes. In addition, predicting the motion patterns of the target based on its trajectory in history is also a promising way worth to explore.

## 7 MOT TRACK

The MOT track aims to recover the trajectories of objects in video sequences, which is an important problem in computer vision with many applications, such as surveillance, activity analysis, and sport video analysis. In the VisDrone-2018 challenge, we divide this track into two sub-tracks depending on whether using prior detection results in individual frames. Specifically, for one sub-track, a submitted algorithm is required to recover the trajectories of objects in video sequences without taking the object detection results as input. The evaluation protocol presented in [93] (*i.e.*, the average precision (AP) of trajectories per object class) is used to evaluate the performance of trackers. In contrast, for the second sub-track, prior object detection results in individual frames are provided and the participating algorithm can work on top of the input detections. In the VisDrone-2019 challenge, we merge these two tracks, and do not distinguish submitted algorithms according to whether they use object detection in each video frame as input or not. The average precision (AP) of the recovered trajectories in [93] is used to evaluate the performance of submitted trackers. Notably, this track uses the same data as the VID track. Specifically, five categories of objects (*i.e.*, *pedestrian*, *car*, *van*, *bus*, and *truck*) in 96 video clips are considered in evaluation.

### 7.1 Evaluation Protocol

In the VisDrone-2018 challenge, the MOT track is divided into two sub-tracks depending on whether prior detection results are used in individual frames. For the multi-object tracking without input detections, we use the metrics in [93] to evaluate the performance. Specifically, we sort the predicted tracklets from algorithms based on the average confidence of the detections of the same identity. If the intersection over union (IoU) overlap between the tracklet and the corresponding ground-truth is larger than a threshold, we regard it as a correct one. Following [93], we average the mean average precision (mAP) per object class over three different thresholds (*i.e.*, 0.25, 0.50, and 0.75) to rank the algorithms. For multi-object tracking with input detections, we use the CLEAR-MOT metrics in [39] in evaluation, *i.e.*, MOTA, MOTP, IDF1, FAF, MT, ML, FP, FN, IDS, and FM. The MOTA metric is the comprehensive metric including three kinds of errors, *i.e.*, FP, FN and IDS. The MOTP metric calculates the average dissimilarity between all true

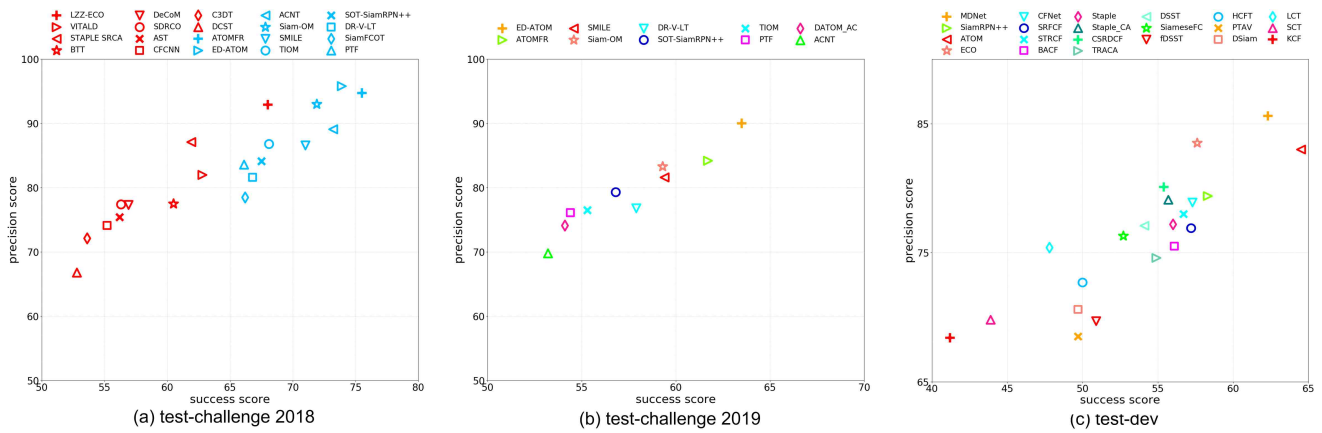


Fig. 8: (a) The success *vs.* precision scores of the top 10 trackers in the VisDrone-SOT 2018 (denoted as red marks) and VisDrone-SOT 2019 (denoted as blue marks) challenges on the `test-challenge 2018` set. The trackers in the VisDrone-SOT 2018 and VisDrone-SOT 2019 challenges are presented in the red and blue markers, respectively. (b) The success *vs.* precision scores of the top 10 trackers in the VisDrone-SOT 209 challenge on the `test-challenge 2019` set. (c) The success *vs.* precision scores of the state-of-the-art trackers on the `test-dev` set.

TABLE 7: Teams participating in VisDrone-MOT 2018 and 2019 challenges, ordered alphabetically.

Codename	AP	MOTA	Institutions	Contributors and References
VisDrone-2018 Challenge:				
Crtrack	16.12	30.80	Centre for Res. & Tech. Hellas	E. Michail, K. Avgerinakis, P. Giannakeris, S. Vrochidis, I. Kompatsiaris [168]
deep-sort_d2	10.47	-	Beijing Univ. of Posts & Telecom.	J. Zhao, Y. Zhao [57], [169]
FRMOT	-	33.10	Autonomous Univ. of Madrid	E. Luna, D. Ortego, J. Miguel, J. Martínez [55]
GOG_EOC	-	36.90	Harbin Inst. of Tech.*, Univ. of Chinese Acad. of Sci. <sup>†</sup>	H. Yu*, G. Li <sup>†</sup> , Q. Huang <sup>†</sup> [170]
MAD	7.27	-	Xidian Univ.	W. Song, Y. Li, Z. Pi, W. Zhang [60], [118]
SCTrack	-	35.80	Univ. of Missouri-Columbia*, U.S. Naval Res. Lab. <sup>†</sup>	N. Al-Shakarji*, F. Bunyak*, G. Seetharaman <sup>†</sup> , K. Palaniappan* [171]
TrackCG	-	42.60	Karlsruhe Inst. of Tech.	W. Tian, Z. Ma, M. Lauer [172]
V-IOU	-	40.20	Berlin Inst. of Tech.	E. Bochinski, T. Senst, T. Sikora [173]
VisDrone-2019 Challenge:				
DBAI-Tracker	43.94	-	DeepBlue Tech. (shanghai)	Z. Luo, Y. Yao, Z. Xu, F. Ni, B. Dong [61], [114], [170], [173]
Flow-Tracker	30.87	-	Xi'an Jiaotong Univ.	W. Li, J. Mu, G. Liu [61], [173], [174]
GGDTRACK	23.09	-	Axis Communications*, Centre for Mathematical Sci. <sup>†</sup>	H. Ardo*, M. Nilsson <sup>†</sup> [55], [175]
HMTT	28.67	-	Beijing Univ. of Posts and Telecom.	S. Pan, Z. Tong, Y. Zhao [64], [124], [173], [176]
IITD_DeepSort	13.88	-	Indian Inst. of Info. Tech.*, Indian Inst. of Tech. <sup>†</sup>	A. Jadhav*, P. Mukherjee*, V. Kaushik <sup>†</sup> , B. Lall <sup>†</sup> [57], [177]
OS-MOT	0.16	-	Univ. of Ottawa*, Shanghai Jiao Tong Univ. <sup>†</sup> , YUNEEC Aviation Tech. <sup>†</sup> , Inst. of Info. Engrg. Chinese Acad. of Sci. <sup>†</sup> , INSKY Lab, Leotail Intell. Tech. <sup>†</sup>	Y. Wang*, L. Ding <sup>†</sup> , R. Laganière*, Z. Sun <sup>†</sup> , C. Zhang <sup>†</sup> , W. Shi <sup>†</sup> [178]
SCTrack	10.09	-	Univ. of Tech.*, Univ. of Missouri-Columbia <sup>†</sup> , U.S. Naval Res. Lab. <sup>†</sup>	N. Al-Shakarji* <sup>†</sup> , F. Bunyak <sup>†</sup> , G. Seetharaman <sup>†</sup> , K. Palaniappan <sup>†</sup> [55], [171]
SGAN	2.54	-	Harbin Inst. of Tech.*, Univ. of Chinese Acad. of Sci. <sup>†</sup>	H. Yu*, G. Li <sup>†</sup> , Q. Huang* <sup>†</sup> [179]
T&D-OF	12.37	-	Dalian Univ. of Tech.	X. Zhang, X. Chen, S. Chen, C. Liu, D. Wang, H. Lu [63], [180], [181]
TNT_DRONE	27.32	-	Univ. of Washington*, Beijing Univ. of Posts and Telecom. <sup>†</sup>	H. Zhang*, Y. Zhang <sup>†</sup> , G. Wang*, J. Hwang* [182]
TrackKITSY	39.19	-	Karlsruhe Inst. of Tech.*, Sun Yat-sen Univ. <sup>†</sup>	W. Tian*, J. Hu <sup>†</sup> , Y. Song*, Z. Chen <sup>†</sup> , L. Chen <sup>†</sup> , M. Lauer* [61], [183]
VCLDAN	7.5	-	Tsinghua Univ.	Z. Xiao [184]

positives and the corresponding ground-truths. The IDF1 metric indicates the ratio of correctly identified detections over the average number of ground truth and computed detections. The FAF metric indicates the average number of false alarms per frame. The FP metric describes the total number of tracker outputs which are the false alarms, and FN is the total number of targets missed by any tracked trajectories in each frame. The IDS metric describes the total number of times that the matched identity of a tracked trajectory changes, while FM is the times that trajectories are disconnected. Both the IDS and FM metrics reflect the accuracy of tracked trajectories. The ML and MT metrics measure the percentage of tracked trajectories less than 20% and more than 80% of the time span based on the ground-

truth respectively.

In VisDrone-2019, we do not distinguish submitted algorithms according to whether they use object detection in each video frame as input or not. Similar to the evaluation protocol used in the multi-object tracking without input detections in the VisDrone-2018 challenge, we use the protocol in [93] to evaluate the performance of algorithms.

## 7.2 Brief Review of MOT Algorithms

Some researchers directly extend the single object tracking algorithms to complete multi-object tracking, such as particle filters [185] and Kalman filters [186], *i.e.*, track each target using an individual single-object tracker. The tracking-by-detection paradigm become popular in multi-object tracking due to its superior performance, which formulates the tracking task as the data association problem, solved by different optimization methods, such as Hungarian algorithm [169], [187], [188], max-flow min-cut [170], energy minimization [189], [190], Markov decision processes [191], and graph optimization [192], [193].

To further improve the performance, recent methods leverage deep networks to exploit discriminative appearance [184], [194], [195] and motion information [196], [197], [198] of targets. A recent trend in multi-object tracking field is to integrate object detection and tracking into a unified framework to share information, such as Tracktor [199] and CenterTrack [200]. Besides the challenging factors (*e.g.*, occlusion, similar appearance and clutter backgrounds) in conventional tracking scenarios, the limitation of computational resource is another factor challenging the performance of tracking algorithms in drone-based applications.

## 7.3 Submitted Algorithms

**VisDrone 2018 challenge.** There are 8 multi-object tracking algorithms submitted in this track [31], shown in Table 7. Crtrack aggregates the predicted events in grouped targets and uses the temporal constraints to stitch short tracklets [168]. V-IOU [173] uses the spatial overlap to associate input detections in consecutive frames. GOG\_EOC develops a

TABLE 8: Comparisons results of the algorithms on the VisDrone-MOT dataset using the evaluation protocol in [93].

Method	AP	AP@0.25	AP@0.50	AP@0.75	AP <sub>car</sub>	AP <sub>bus</sub>	AP <sub>trk</sub>	AP <sub>ped</sub>	AP <sub>van</sub>
VisDrone-2018 challenge:									
Ctrack	<b>16.12</b>	<b>22.40</b>	<b>16.26</b>	<b>9.70</b>	27.74	28.45	8.15	7.95	8.31
deep-sort_d2	10.47	17.26	9.40	4.75	<b>29.14</b>	2.38	3.46	7.12	<b>10.25</b>
MAD	7.27	12.72	7.03	2.07	16.23	1.65	2.85	<b>14.16</b>	1.46
VisDrone-2019 challenge:									
DBAI-Tracker	<b>43.94</b>	<b>57.32</b>	<b>45.18</b>	29.32	<b>55.13</b>	<b>44.97</b>	<b>42.73</b>	31.01	<b>45.85</b>
TrackKITSY	39.19	48.83	39.36	<b>29.37</b>	54.92	29.05	34.19	<b>36.57</b>	41.20
Flow-Tracker	30.87	41.84	31.00	19.77	48.44	26.19	29.50	18.65	31.56
HMTT	28.67	39.05	27.88	19.08	44.35	30.56	18.75	26.49	23.19
TNT_DRONE	27.32	35.09	26.92	19.94	38.06	22.65	33.79	12.62	29.46
GGDTRACK	23.09	31.01	22.70	15.55	35.45	28.57	11.90	17.20	22.34
IITD_DeepSort	13.88	23.19	12.81	5.64	32.20	8.83	6.61	18.61	3.16
T&D-OF	12.37	17.74	12.94	6.43	23.31	22.02	2.48	9.59	4.44
SCTrack	10.09	14.95	9.41	5.92	18.98	17.86	4.86	5.20	3.58
VCLDAN	7.50	10.75	7.41	4.33	21.63	0.00	4.92	10.94	0.00
VisDrone-dev:									
GOG [170]	<b>5.14</b>	<b>11.02</b>	3.25	1.14	<b>13.70</b>	<b>3.09</b>	1.94	3.08	3.87
IOUT [173]	4.34	8.32	<b>3.29</b>	1.40	10.90	2.15	<b>2.53</b>	1.98	<b>4.11</b>
SORT [169]	3.37	5.78	2.82	<b>1.50</b>	8.30	1.04	2.47	0.95	4.06
MOTDT [181]	1.22	2.43	0.92	0.30	0.36	0.00	0.15	<b>5.08</b>	0.49

context harmony model to create exchanging object context patches via the Siamese network, and tracks the objects using the algorithm in [170]. SCTrack [171] uses a color correlation cost matrix to maintain object identities. TrackCG [172] achieves the best performance with MOTA score 42.60 among all trackers using the public input detections. It first estimates the target state using the motion pattern of grouped objects to build short tracklets, and uses the graph model to generate long trajectories. Two other methods use private input detections, *i.e.*, MAD, using YOLOv3 [60] for detection and CFNet [118]) for association, and deep-sort\_v2, using RetinaNet [57] for detection and Deep-SORT [169]) for association.

**VisDrone 2019 challenge.** In this track [33], we have received 12 entries for 23 different institutes, shown in Table 7. Most of the submissions are based on the tracking-by-detection framework, *i.e.*, the trackers exploit temporal coherence to associate detections in individual frames to recover the trajectories of targets. At first, several submissions use the state-of-the-art detectors, such as R-FCN [63], RetinaNet [57], Cascade R-CNN [61], and CenterNet [64] to generate object detections in individual frames. After that, some submitted methods use the single object tracking methods, such as KCF [114] and DaSiameseRPN [124], to recover false negatives of detectors. Some other methods, such as GGDTRACK, Flow-Tracker, OS-MOT, T&D-OF, TrackKITSY, and SGAN, attempt to exploit low-level or middle-level temporal information to improve the tracking performance. The HMTT, IITD\_DeepSort, SCTrack, T&D-OF, TNT\_DRONE, and VCLDCN methods use the metric learning algorithms to compute the similarities between detections in consecutive frames, which is effective in occlusion and miss detection challenges.

**VisDrone-dev benchmark.** We evaluate 4 multi-object tracking methods in this track for comparison, including GOG [170], IOUT [173], SORT [169] and MOTDT [181]. Notably, the FPN [58] object detection method is used to generate the input detections in each individual frame.

## 7.4 Results and Analysis

**Results on the test-challenge set.** We report the evaluation results of the trackers in the VisDrone-VDT 2018

TABLE 9: Comparisons results of the algorithms on the VisDrone-MOT dataset using the CLEAR-MOT evaluation protocol [39].

Method	MOTA	MOTP	IDF1	FAF	MT	ML	FP	FN	IDS	FM
VisDrone-2018 challenge:										
TrackCG	<b>42.6</b>	74.1	<b>58.0</b>	0.86	323	395	14722	68060	779	3717
V-IOU	40.2	74.9	56.1	0.76	297	514	11838	74027	<b>265</b>	1380
GOG_EOC	36.9	<b>75.8</b>	46.5	<b>0.29</b>	205	589	<b>5445</b>	86399	354	<b>1090</b>
SCTrack	35.8	75.6	45.1	0.39	211	550	7298	85623	798	2042
FRMOT	33.1	73.0	50.8	1.15	254	463	21736	74953	1043	2534
Ctrack	30.8	73.5	51.9	1.95	<b>369</b>	<b>375</b>	36930	<b>62819</b>	1376	2190
VisDrone-dev:										
GOG [170]	<b>28.7</b>	<b>76.1</b>	36.4	<b>0.78</b>	346	836	<b>17706</b>	144657	<b>1387</b>	<b>2237</b>
IOUT [173]	28.1	74.7	<b>38.9</b>	1.60	467	670	36158	126549	2393	3829
SORT [169]	14.0	73.2	<b>38.0</b>	<b>3.57</b>	<b>506</b>	<b>545</b>	80845	<b>112954</b>	3629	4838
MOTDT [181]	-0.8	68.5	21.6	1.97	87	1196	44548	185453	1437	3609

[31] and VisDrone-MOT 2019 [33] challenges with the evaluation protocols [93] and [39] in Table 8 and 9, respectively. As shown in Table 8, in the subtrack without using prior input detections in the VisDrone-VDT 2018 challenge, Ctrack achieves the best AP score 16.12% by aggregating the prediction events in grouped targets and stitching the tracks by temporal constraints. In this way, the targets in crowded scenarios are able to be recovered after being occluded. In the VisDrone-MOT 2019 Challenge, the submitted algorithms achieve significant improvements, *e.g.*, DBAI-Tracker improves the top AP score by 27.82%, *i.e.*, 43.94% *vs.* 16.12%. Notably, the top three trackers, *i.e.*, DBAI-Tracker, TrackKITSY and Flow-Tracker, use Cascade R-CNN [61] to generate detections in individual frames, and integrate the temporal information, *e.g.*, FlowNet [174] and IoU tracker [173] to complete association. Similarly, HMTT combines CenterNet [64], IoU tracker [173] and DaSiameseRPN [124] for multiple object tracking, ranked in the fourth place in the challenge.

For the sub-track using provided input detections, *i.e.*, generated by Faster R-CNN [55] in the VisDrone-MOT 2018 challenge, TrackCG achieves the best MOTA and IDF1 scores. V-IOU achieves slightly inferior MOTA and IDF1 scores than TrackCG, but produces the best IDS score, *i.e.*, 265. It associates detections based on spatial overlap, *i.e.*, intersection-over-union, in consecutive frames. We speculate that the overlapping based measurement is reliable enough in drone captured videos from high altitude, which do not contain large displacements of objects. GOG\_EOC obtains the best FAF, FP and FM scores, *i.e.*, 0.29, 5, 445, and 1,090, which uses both the detection overlap and context harmony degree to measure the similarities between detections in consecutive frames. SCTrack designs a color correlation cost matrix to maintain object identities. However, the color information is not reliable enough, resulting in inferior results, *i.e.*, ranked in the fourth place in terms of MOTA (35.8). FRMOT is an online tracker using the Hungarian algorithm for associating detections, leading to relative large IDS (1,043) and FM (2,534) scores.

**Results on the test-dev set.** We evaluate 4 multi-object tracking on the test-dev set with the evaluation protocols [93] and [39], shown in Table 8 and 9, respectively. Notably, FPN [58] is used to generate object detections in individual frames for the sub-track using prior input detections.

GOG [170] and IOUT [173] benefit from global information of whole sequences and spatial overlap between frame detections, achieving the best tracking results in terms of

both evaluation protocols [93] and [39]. SORT [169] approximates the inter-frame displacements of each object with a linear constant velocity model, which is independent of object categories and camera motion, significantly degrading its performance. MOTDT [181] computes the similarities between objects using appearance model trained on other large-scale person re-identification datasets without fine-tuning, leading to inferior accuracy.

## 7.5 Discussion

Most of the MOT algorithms formulate the tracking task as a data association problem, which aims to associate object detections in individual frames to generate object trajectories. Thus, the accuracy of object detection in individual frames significantly influence the performance of MOT. Intuitively, integrating object detection and tracking into a unified framework is promising to improve the performance. In the following, we discuss two potential research directions to further boost the performance.

**Similarity calculation.** For the data association problem, similarity computation between different detections in individual frames is crucial for the tracking performance. The appearance and motion information should be considered in computing the similarities. For example, a Siamese network offline trained on the ImageNet VID dataset [3] can be used to exploit temporal discriminative features of objects. The Siamese network can be fine-tuned in tracking process to further improve the accuracy. Meanwhile, several low-level and mid-level motion features are also effective and useful for the MOT algorithms, such as KLT and optical flow.

**Scene understanding.** is another effective way to improve the MOT performance. For example, based on the scene understanding module, we can infer the enter or exit ports in the scenes. The information of the enter and exit ports is a strong priori for the trackers to distinguish occlusion, termination, or re-appearing of the target. Meanwhile, the tracker is also able to suppress false trajectories based on general knowledge and scene understanding, *e.g.*, the vehicles are only driven on the road rather on the building. In summary, this area is worth further studying to improve the MOT performance.

## 8 CONCLUSION

We introduce a new large-scale benchmark, **VisDrone**, to facilitate the research of object detection and tracking on drone captured imagery. With over 6,000 worker hours, a vast collection of object instances are gathered, annotated, and organized to drive the advancement of object detection and tracking algorithms. We place emphasis on capturing images and video clips in real life environments. Notably, the dataset is recorded over 14 different cities in China with various drone platforms, featuring a diverse real-world scenarios. We provide a rich set of annotations including more than 2.5 million annotated instances along with several important attributes. The **VisDrone** benchmark is made available to the research community through the project website: [www.aiskyeye.com](http://www.aiskyeye.com). The best submissions in the four tracks are still far from satisfactory in real applications.

## ACKNOWLEDGEMENTS

We would like to thank Jiayu Zheng and Tao Peng for valuable and constructive suggestions to improve the quality of this paper.

## REFERENCES

- [1] P. Dollár, C. Wojek, B. Schiele, and P. Perona, "Pedestrian detection: An evaluation of the state of the art," *TPAMI*, vol. 34, no. 4, pp. 743–761, 2012.
- [2] A. Geiger, P. Lenz, and R. Urtasun, "Are we ready for autonomous driving? the KITTI vision benchmark suite," in *CVPR*, 2012, pp. 3354–3361.
- [3] O. Russakovsky, J. Deng, H. Su, J. Krause, S. Satheesh, S. Ma, Z. Huang, A. Karpathy, A. Khosla, M. S. Bernstein, A. C. Berg, and F. Li, "Imagenet large scale visual recognition challenge," *IJCV*, vol. 115, no. 3, pp. 211–252, 2015.
- [4] T. Lin, M. Maire, S. J. Belongie, J. Hays, P. Perona, D. Ramanan, P. Dollár, and C. L. Zitnick, "Microsoft COCO: common objects in context," in *ECCV*, 2014, pp. 740–755.
- [5] Y. Wu, J. Lim, and M. Yang, "Object tracking benchmark," *TPAMI*, vol. 37, no. 9, pp. 1834–1848, 2015.
- [6] L. Cehovin, A. Leonardis, and M. Kristan, "Visual object tracking performance measures revisited," *TIP*, vol. 25, no. 3, pp. 1261–1274, 2016.
- [7] L. Leal-Taixé, A. Milan, I. D. Reid, S. Roth, and K. Schindler, "Motchallenge 2015: Towards a benchmark for multi-target tracking," *CoRR*, vol. abs/1504.01942, 2015.
- [8] L. Wen, D. Du, Z. Cai, Z. Lei, M. Chang, H. Qi, J. Lim, M. Yang, and S. Lyu, "UA-DETRAC: A new benchmark and protocol for multi-object detection and tracking," *Computer Vision and Image Understanding*, 2020.
- [9] H. Fan, L. Lin, F. Yang, P. Chu, G. Deng, S. Yu, H. Bai, Y. Xu, C. Liao, and H. Ling, "Lasot: A high-quality benchmark for large-scale single object tracking," *CoRR*, vol. abs/1809.07845, 2018.
- [10] M. Mueller, N. Smith, and B. Ghanem, "A benchmark and simulator for UAV tracking," in *ECCV*, 2016, pp. 445–461.
- [11] M. Hsieh, Y. Lin, and W. H. Hsu, "Drone-based object counting by spatially regularized regional proposal network," in *ICCV*, 2017.
- [12] A. Robicquet, A. Sadeghian, A. Alahi, and S. Savarese, "Learning social etiquette: Human trajectory understanding in crowded scenes," in *ECCV*, 2016, pp. 549–565.
- [13] M. Everingham, L. Van Gool, C. K. I. Williams, J. Winn, and A. Zisserman, "The PASCAL Visual Object Classes Challenge 2012 (VOC2012) Results," <http://www.pascal-network.org/challenges/VOC/voc2012/workshop/index.html>, 2012.
- [14] S. Razakarivony and F. Jurie, "Vehicle detection in aerial imagery: A small target detection benchmark," *Journal of Visual Communication and Image Representation*, vol. 34, pp. 187–203, 2016.
- [15] T. N. Mundhenk, G. Konjevod, W. A. Sakla, and K. Boakye, "A large contextual dataset for classification, detection and counting of cars with deep learning," in *ECCV*, 2016, pp. 785–800.
- [16] G. Xia, X. Bai, J. Ding, Z. Zhu, S. J. Belongie, J. Luo, M. Datcu, M. Pelillo, and L. Zhang, "DOTA: A large-scale dataset for object detection in aerial images," in *CVPR*, 2018, pp. 3974–3983.
- [17] A. Milan, L. Leal-Taixé, K. Schindler, D. Cremers, S. Roth, and I. D. Reid, "MOT17 Challenge," <https://motchallenge.net/>, 2017.
- [18] M. Berekatain, M. Martí, H. Shih, S. Murray, K. Nakayama, Y. Matsuo, and H. Prendinger, "Okutama-action: An aerial view video dataset for concurrent human action detection," in *CVPR Workshops*, 2017, pp. 2153–2160.
- [19] D. Du, Y. Qi, H. Yu, Y. Yang, K. Duan, G. Li, W. Zhang, Q. Huang, and Q. Tian, "The unmanned aerial vehicle benchmark: Object detection and tracking," in *ECCV*, 2018, pp. 375–391.
- [20] I. Kalra, M. Singh, S. Nagpal, R. Singh, M. Vatsa, and P. B. Sujit, "Dronesurf: Benchmark dataset for drone-based face recognition," in *FG*, 2019, pp. 1–7.
- [21] A. W. M. Smeulders, D. M. Chu, R. Cucchiara, S. Calderara, A. Dehghan, and M. Shah, "Visual tracking: An experimental survey," *TPAMI*, vol. 36, no. 7, pp. 1442–1468, 2014.
- [22] P. Liang, E. Blasch, and H. Ling, "Encoding color information for visual tracking: Algorithms and benchmark," *TIP*, vol. 24, no. 12, pp. 5630–5644, 2015.

- [23] M. Kristan, A. Leonardis, J. Matas, M. Felsberg, R. P. Pflugfelder, L. Cehovin, T. Vojir, G. Häger, A. Lukežic, G. Fernández, and *et al.*, “The visual object tracking VOT2016 challenge results,” in *ECCVWorkshops*, 2016, pp. 777–823.
- [24] H. K. Galoogahi, A. Fagg, C. Huang, D. Ramanan, and S. Lucey, “Need for speed: A benchmark for higher frame rate object tracking,” in *ICCV*, 2017, pp. 1134–1143.
- [25] P. Liang, Y. Wu, H. Lu, L. Wang, C. Liao, and H. Ling, “Planar object tracking in the wild: A benchmark,” in *ICRA*, 2018, pp. 651–658.
- [26] E. Ristani, F. Solera, R. S. Zou, R. Cucchiara, and C. Tomasi, “Performance measures and a data set for multi-target, multi-camera tracking,” in *ECCVWorkshops*, 2016, pp. 17–35.
- [27] P. Zhu, L. Wen, D. Du, X. Bian, H. Ling, Q. Hu, and *et al.*, “Visdrone-det2018: The vision meets drone object detection in image challenge results,” in *ECCV Workshops*, 2018, pp. 437–468.
- [28] D. Du, P. Zhu, L. Wen, X. Bian, H. Ling, Q. Hu, and *et al.*, “Visdrone-det2019: The vision meets drone object detection in image challenge results,” in *ICCV Workshops*, 2019.
- [29] L. Wen, P. Zhu, D. Du, X. Bian, H. Ling, Q. Hu, and *et al.*, “Visdrone-sot2018: The vision meets drone single-object tracking challenge results,” in *ECCV Workshops*, 2018, pp. 469–495.
- [30] D. Du, P. Zhu, L. Wen, X. Bian, H. Ling, Q. Hu, and *et al.*, “Visdrone-sot2019: The vision meets drone single object tracking challenge results,” in *ICCV Workshops*, 2019.
- [31] P. Zhu, L. Wen, D. Du, X. Bian, H. Ling, Q. Hu, and *et al.*, “Visdrone-vdt2018: The vision meets drone video detection and tracking challenge results,” in *ECCV Workshops*, 2018, pp. 496–518.
- [32] P. Zhu, D. Du, L. Wen, X. Bian, H. Ling, Q. Hu, and *et al.*, “Visdrone-vid2019: The vision meets drone object detection in video challenge results,” in *ICCV Workshops*, 2019.
- [33] L. Wen, P. Zhu, D. Du, X. Bian, H. Ling, Q. Hu, and *et al.*, “Visdrone-mot2019: The vision meets drone multiple object tracking challenge results,” in *ICCV Workshops*, 2019.
- [34] M. Everingham, L. J. V. Gool, C. K. I. Williams, J. M. Winn, and A. Zisserman, “The pascal visual object classes (VOC) challenge,” *IJCV*, vol. 88, no. 2, pp. 303–338, 2010.
- [35] M. Everingham, S. M. A. Eslami, L. J. V. Gool, C. K. I. Williams, J. M. Winn, and A. Zisserman, “The pascal visual object classes challenge: A retrospective,” *IJCV*, vol. 111, no. 1, pp. 98–136, 2015.
- [36] J. Deng, W. Dong, R. Socher, L. Li, K. Li, and F. Li, “Imagenet: A large-scale hierarchical image database,” in *CVPR*, 2009, pp. 248–255.
- [37] S. Lyu, M. Chang, D. Du, L. Wen, H. Qi, Y. Li, Y. Wei, L. Ke, T. Hu, M. D. Cocco, P. Carcagni, and *et al.*, “UA-DETRAC 2017: Report of AVSS2017 & IWT4S challenge on advanced traffic monitoring,” in *AVSS*, 2017, pp. 1–7.
- [38] S. Lyu, M. Chang, D. Du, W. Li, Y. Wei, M. D. Cocco, P. Carcagni, and *et al.*, “UA-DETRAC 2018: Report of AVSS2018 & IWT4S challenge on advanced traffic monitoring,” in *AVSS*, 2018, pp. 1–6.
- [39] A. Milan, L. Leal-Taixé, I. D. Reid, S. Roth, and K. Schindler, “Mot16: A benchmark for multi-object tracking,” *arXiv preprint*, vol. abs/1603.00831, 2016.
- [40] A. Prest, C. Leistner, J. Civera, C. Schmid, and V. Ferrari, “Learning object class detectors from weakly annotated video,” in *CVPR*, 2012, pp. 3282–3289.
- [41] V. Kalogeiton, V. Ferrari, and C. Schmid, “Analysing domain shift factors between videos and images for object detection,” *TPAMI*, vol. 38, no. 11, pp. 2327–2334, 2016.
- [42] Y. Wu, J. Lim, and M. Yang, “Online object tracking: A benchmark,” in *CVPR*, 2013, pp. 2411–2418.
- [43] M. Kristan, A. Leonardis, J. Matas, M. Felsberg, R. P. Pflugfelder, L. C. Zajc, T. Vojir, G. Häger, A. Lukežic, A. Eldesokey, G. Fernández, and *et al.*, “The visual object tracking VOT2017 challenge results,” in *ICCVWorkshops*, 2017, pp. 1949–1972.
- [44] M. Kristan, A. Leonardis, J. Matas, M. Felsberg, R. P. Pflugfelder, L. C. Zajc, T. Vojir, G. Bhat, A. Lukežic, A. Eldesokey, G. Fernández, and *et al.*, “The sixth visual object tracking VOT2018 challenge results,” in *ECCVWorkshops*, 2018, pp. 3–53.
- [45] A. Li, M. Li, Y. Wu, M.-H. Yang, and S. Yan, “NUS-PRO: A new visual tracking challenge,” in *TPAMI*, 2015, pp. 1–15.
- [46] D. Du, H. Qi, W. Li, L. Wen, Q. Huang, and S. Lyu, “Online deformable object tracking based on structure-aware hyper-graph,” *TIP*, vol. 25, no. 8, pp. 3572–3584, 2016.
- [47] M. Felsberg, A. Berg, G. Häger, J. Ahlberg, M. Kristan, J. Matas, A. Leonardis, L. Cehovin, G. Fernández, T. Vojir, G. Nebehay, and R. P. Pflugfelder, “The thermal infrared visual object tracking VOT-TIR2015 challenge results,” in *ICCVWorkshops*, 2015, pp. 639–651.
- [48] M. F. *et al.*, “The thermal infrared visual object tracking VOT-TIR2016 challenge results,” in *ECCVWorkshops*, 2016, pp. 824–849.
- [49] J. Ferryman and A. Shahroki, “Pets2009: Dataset and challenge,” in *AVSS*, 2009, pp. 1–6.
- [50] W. Chen, L. Cao, X. Chen, and K. Huang, “An equalized global graph model-based approach for multicamera object tracking,” *TCSVT*, vol. 27, no. 11, pp. 2367–2381, 2017.
- [51] S. Zhang, E. Staudt, T. Faltemier, and A. K. Roy-Chowdhury, “A camera network tracking (camnet) dataset and performance baseline,” in *WACV*, 2015, pp. 365–372.
- [52] S. Li and D. Yeung, “Visual object tracking for unmanned aerial vehicles: A benchmark and new motion models,” in *AAAI*, 2017, pp. 4140–4146.
- [53] A. Rozantsev, V. Lepetit, and P. Fua, “Detecting flying objects using a single moving camera,” *TPAMI*, vol. 39, no. 5, pp. 879–892, 2017.
- [54] J. Wang, Y. Li, and S. Wang, “A highly accurate feature fusion network for vehicle detection in surveillance scenarios,” in *BMVC*, 2018, p. 217.
- [55] S. Ren, K. He, R. B. Girshick, and J. Sun, “Faster R-CNN: towards real-time object detection with region proposal networks,” *TPAMI*, vol. 39, no. 6, pp. 1137–1149, 2017.
- [56] W. Liu, D. Anguelov, D. Erhan, C. Szegedy, S. E. Reed, C. Fu, and A. C. Berg, “SSD: single shot multibox detector,” in *ECCV*, 2016, pp. 21–37.
- [57] T. Lin, P. Goyal, R. B. Girshick, K. He, and P. Dollár, “Focal loss for dense object detection,” in *ICCV*, 2017, pp. 2999–3007.
- [58] T. Lin, P. Dollár, R. B. Girshick, K. He, B. Hariharan, and S. J. Belongie, “Feature pyramid networks for object detection,” in *CVPR*, 2017, pp. 936–944.
- [59] Z. Li, C. Peng, G. Yu, X. Zhang, Y. Deng, and J. Sun, “Light-head R-CNN: in defense of two-stage object detector,” *CoRR*, vol. abs/1711.07264, 2017.
- [60] J. Redmon and A. Farhadi, “Yolov3: An incremental improvement,” *CoRR*, vol. abs/1804.02767, 2018.
- [61] Z. Cai and N. Vasconcelos, “Cascade R-CNN: delving into high quality object detection,” in *CVPR*, 2018, pp. 6154–6162.
- [62] S. Zhang, L. Wen, X. Bian, Z. Lei, and S. Z. Li, “Single-shot refinement neural network for object detection,” in *CVPR*, 2018, pp. 4203–4212.
- [63] J. Dai, Y. Li, K. He, and J. Sun, “R-FCN: object detection via region-based fully convolutional networks,” in *NeurIPS*, 2016, pp. 379–387.
- [64] X. Zhou, D. Wang, and P. Krähenbühl, “Objects as points,” *CoRR*, vol. abs/1904.07850, 2019.
- [65] Y. Wu, Z. Cheng, Z. Xu, and W. Wang, “Segmentation is all you need,” *CoRR*, vol. abs/1904.13300, 2019.
- [66] K. Sun, B. Xiao, D. Liu, and J. Wang, “Deep high-resolution representation learning for human pose estimation,” *CoRR*, vol. abs/1902.09212, 2019.
- [67] K. Chen, J. Pang, J. Wang, Y. Xiong, X. Li, S. Sun, W. Feng, Z. Liu, J. Shi, W. Ouyang, C. C. Loy, and D. Lin, “Hybrid task cascade for instance segmentation,” in *CVPR*, 2019.
- [68] B. Singh, M. Najibi, and L. S. Davis, “SNIPER: efficient multi-scale training,” in *NeurIPS*, 2018, pp. 9333–9343.
- [69] J. Pang, K. Chen, J. Shi, H. Feng, W. Ouyang, and D. Lin, “Libra R-CNN: towards balanced learning for object detection,” in *CVPR*, 2019.
- [70] C. Yu, J. Wang, C. Peng, C. Gao, G. Yu, and N. Sang, “Learning a discriminative feature network for semantic segmentation,” in *CVPR*, 2018, pp. 1857–1866.
- [71] Y. Li, Y. Chen, N. Wang, and Z. Zhang, “Scale-aware trident networks for object detection,” *CoRR*, vol. abs/1901.01892, 2019.
- [72] J. Wang, K. Chen, S. Yang, C. C. Loy, and D. Lin, “Region proposal by guided anchoring,” *CoRR*, vol. abs/1901.03278, 2019.
- [73] P. A. Viola and M. J. Jones, “Robust real-time face detection,” *IJCV*, vol. 57, no. 2, pp. 137–154, 2004.
- [74] N. Dalal and B. Triggs, “Histograms of oriented gradients for human detection,” in *CVPR*, 2005, pp. 886–893.
- [75] P. F. Felzenszwalb, D. A. McAllester, and D. Ramanan, “A discriminatively trained, multiscale, deformable part model,” in *CVPR*, 2008.

- [76] P. Dollár, R. Appel, S. J. Belongie, and P. Perona, "Fast feature pyramids for object detection," *TPAMI*, vol. 36, no. 8, pp. 1532–1545, 2014.
- [77] P. Dollár, Z. Tu, P. Perona, and S. J. Belongie, "Integral channel features," in *BMVC*, A. Cavallaro, S. Prince, and D. C. Alexander, Eds., 2009, pp. 1–11.
- [78] R. B. Girshick, J. Donahue, T. Darrell, and J. Malik, "Rich feature hierarchies for accurate object detection and semantic segmentation," in *CVPR*, 2014, pp. 580–587.
- [79] K. He, X. Zhang, S. Ren, and J. Sun, "Spatial pyramid pooling in deep convolutional networks for visual recognition," *TPAMI*, vol. 37, no. 9, pp. 1904–1916, 2015.
- [80] R. B. Girshick, "Fast R-CNN," in *ICCV*, 2015, pp. 1440–1448.
- [81] K. He, G. Gkioxari, P. Dollár, and R. B. Girshick, "Mask R-CNN," in *ICCV*, 2017, pp. 2980–2988.
- [82] J. Redmon, S. K. Divvala, R. B. Girshick, and A. Farhadi, "You only look once: Unified, real-time object detection," in *CVPR*, 2016, pp. 779–788.
- [83] J. Redmon and A. Farhadi, "YOLO9000: better, faster, stronger," in *CVPR*, 2017, pp. 6517–6525.
- [84] H. Law and J. Deng, "Cornernet: Detecting objects as paired keypoints," in *ECCV*, 2018, pp. 765–781.
- [85] Z. Tian, C. Shen, H. Chen, and T. He, "FCOS: fully convolutional one-stage object detection," in *ICCV*, 2019, pp. 9626–9635.
- [86] C. Zhu, Y. He, and M. Savvides, "Feature selective anchor-free module for single-shot object detection," in *CVPR*, 2019, pp. 840–849.
- [87] J. Hu, L. Shen, and G. Sun, "Squeeze-and-excitation networks," in *CVPR*, 2018.
- [88] F. Wang, M. Jiang, C. Qian, S. Yang, C. Li, H. Zhang, X. Wang, and X. Tang, "Residual attention network for image classification," in *CVPR*, 2017, pp. 6450–6458.
- [89] Y. Cao, J. Xu, S. Lin, F. Wei, and H. Hu, "Gnet: Non-local networks meet squeeze-excitation networks and beyond," *CoRR*, vol. abs/1904.11492, 2019.
- [90] J. Dai, H. Qi, Y. Xiong, Y. Li, G. Zhang, H. Hu, and Y. Wei, "Deformable convolutional networks," in *ICCV*, 2017, pp. 764–773.
- [91] Z. Li, C. Peng, G. Yu, X. Zhang, Y. Deng, and J. Sun, "Detnet: Design backbone for object detection," in *ECCV*, 2018, pp. 339–354.
- [92] M. Haris, G. Shakhnarovich, and N. Ukita, "Deep back-projection networks for super-resolution," in *CVPR*, 2018, pp. 1664–1673.
- [93] E. Park, W. Liu, O. Russakovsky, J. Deng, F.-F. Li, and A. Berg, "Large Scale Visual Recognition Challenge 2017," <http://image-net.org/challenges/LSVRC/2017>, 2017.
- [94] M. Danelljan, G. Bhat, F. S. Khan, and M. Felsberg, "ECO: efficient convolution operators for tracking," in *CVPR*, 2017, pp. 6931–6939.
- [95] X. Zhu, Y. Wang, J. Dai, L. Yuan, and Y. Wei, "Flow-guided feature aggregation for video object detection," in *ICCV*, 2017, pp. 408–417.
- [96] H. Law, Y. Teng, O. Russakovsky, and J. Deng, "Cornernet-lite: Efficient keypoint based object detection," *CoRR*, vol. abs/1904.08900, 2019.
- [97] Q. Zhao, T. Sheng, Y. Wang, Z. Tang, Y. Chen, L. Cai, and H. Ling, "M2det: A single-shot object detector based on multi-level feature pyramid network," in *AAAI*, 2019, pp. 9259–9266.
- [98] M. Danelljan, G. Bhat, F. S. Khan, and M. Felsberg, "ECO: efficient convolution operators for tracking," in *CVPR*, 2017, pp. 6931–6939.
- [99] B. Li, W. Wu, Q. Wang, F. Zhang, J. Xing, and J. Yan, "Siamrpn++: Evolution of siamese visual tracking with very deep networks," in *CVPR*, 2018.
- [100] B. Zoph, E. D. Cubuk, G. Ghiasi, T. Lin, J. Shlens, and Q. V. Le, "Learning data augmentation strategies for object detection," *CoRR*, vol. abs/1906.11172, 2019.
- [101] X. Wang, G. Hua, and T. X. Han, "Detection by detections: Non-parametric detector adaptation for a video," in *CVPR*, 2012, pp. 350–357.
- [102] X. Zhu, Y. Xiong, J. Dai, L. Yuan, and Y. Wei, "Deep feature flow for video recognition," in *CVPR*, 2017, pp. 4141–4150.
- [103] F. Xiao and Y. J. Lee, "Video object detection with an aligned spatial-temporal memory," in *ECCV*, vol. 11212, 2018, pp. 494–510.
- [104] W. Han, P. Khorrami, T. L. Paine, P. Ramachandran, M. Babaeizadeh, H. Shi, J. Li, S. Yan, and T. S. Huang, "Seq-nms for video object detection," *CoRR*, vol. abs/1602.08465, 2016.
- [105] C. Feichtenhofer, A. Pinz, and A. Zisserman, "Detect to track and track to detect," in *ICCV*, 2017, pp. 3057–3065.
- [106] K. Kang, H. Li, J. Yan, X. Zeng, B. Yang, T. Xiao, C. Zhang, Z. Wang, R. Wang, X. Wang, and W. Ouyang, "T-CNN: tubelets with convolutional neural networks for object detection from videos," *TCSVT*, vol. 28, no. 10, pp. 2896–2907, 2018.
- [107] S. Xie, R. B. Girshick, P. Dollár, Z. Tu, and K. He, "Aggregated residual transformations for deep neural networks," in *CVPR*, 2017, pp. 5987–5995.
- [108] L. Wen, Z. Cai, Z. Lei, D. Yi, and S. Z. Li, "Online spatio-temporal structural context learning for visual tracking," in *ECCV*, 2012, pp. 716–729.
- [109] W. Zhou, L. Wen, L. Zhang, D. Du, T. Luo, and Y. Wu, "Siamman: Siamese motion-aware network for visual tracking," *CoRR*, vol. abs/1912.05515, 2019.
- [110] F. Li, C. Tian, W. Zuo, L. Zhang, and M. Yang, "Learning spatial-temporal regularized correlation filters for visual tracking," in *CVPR*, 2018, pp. 4904–4913.
- [111] H. Nam and B. Han, "Learning multi-domain convolutional neural networks for visual tracking," in *CVPR*, 2016, pp. 4293–4302.
- [112] H. K. Galoogahi, A. Fagg, and S. Lucey, "Learning background-aware correlation filters for visual tracking," in *ICCV*, 2017, pp. 1144–1152.
- [113] Z. He, Y. Fan, J. Zhuang, Y. Dong, and H. Bai, "Correlation filters with weighted convolution responses," in *ICCVWorkshops*, 2017, pp. 1992–2000.
- [114] J. F. Henriques, R. Caseiro, P. Martins, and J. Batista, "High-speed tracking with kernelized correlation filters," *TPAMI*, vol. 37, no. 3, pp. 583–596, 2015.
- [115] Q. Wang, J. Gao, J. Xing, M. Zhang, and W. Hu, "Dcfnet: Discriminant correlation filters network for visual tracking," *CoRR*, vol. abs/1704.04057, 2017.
- [116] L. Bertinetto, J. Valmadre, S. Golodetz, O. Miksik, and P. H. S. Torr, "Staple: Complementary learners for real-time tracking," in *CVPR*, 2016, pp. 1401–1409.
- [117] J. Choi, H. J. Chang, T. Fischer, S. Yun, K. Lee, J. Jeong, Y. Demiris, and J. Y. Choi, "Context-aware deep feature compression for high-speed visual tracking," in *CVPR*, 2018.
- [118] J. Valmadre, L. Bertinetto, J. F. Henriques, A. Vedaldi, and P. H. S. Torr, "End-to-end representation learning for correlation filter based tracking," in *CVPR*, 2017, pp. 5000–5008.
- [119] M. Mueller, N. Smith, and B. Ghanem, "Context-aware correlation filter tracking," in *CVPR*, 2017, pp. 1387–1395.
- [120] Y. Song, C. Ma, X. Wu, L. Gong, L. Bao, W. Zuo, C. Shen, R. W. H. Lau, and M. Yang, "VITAL: visual tracking via adversarial learning," in *CVPR*, 2018.
- [121] M. Danelljan, G. Bhat, F. S. Khan, and M. Felsberg, "ATOM: accurate tracking by overlap maximization," *CoRR*, vol. abs/1811.07628, 2018.
- [122] B. Li, J. Yan, W. Wu, Z. Zhu, and X. Hu, "High performance visual tracking with siamese region proposal network," in *CVPR*, 2018, pp. 8971–8980.
- [123] Z. Zhang, H. Peng, and Q. Wang, "Deeper and wider siamese networks for real-time visual tracking," *CoRR*, vol. abs/1901.01660, 2019.
- [124] Z. Zhu, Q. Wang, B. Li, W. Wu, J. Yan, and W. Hu, "Distractor-aware siamese networks for visual object tracking," in *ECCV*, 2018, pp. 103–119.
- [125] T. Xu, Z. Feng, X. Wu, and J. Kittler, "Learning adaptive discriminative correlation filters via temporal consistency preserving spatial feature selection for robust visual tracking," *CoRR*, vol. abs/1807.11348, 2018.
- [126] D. A. Ross, J. Lim, R. Lin, and M. Yang, "Incremental learning for robust visual tracking," *IJCV*, vol. 77, no. 1-3, pp. 125–141, 2008.
- [127] X. Mei and H. Ling, "Robust visual tracking using  $\ell_1$  minimization," in *ICCV*, 2009, pp. 1436–1443.
- [128] Z. Kalal, J. Matas, and K. Mikolajczyk, "P-N learning: Bootstrapping binary classifiers by structural constraints," in *CVPR*, 2010, pp. 49–56.
- [129] S. Hare, S. Golodetz, A. Saffari, V. Vineet, M. Cheng, S. L. Hicks, and P. H. S. Torr, "Struck: Structured output tracking with kernels," *TPAMI*, vol. 38, no. 10, pp. 2096–2109, 2016.

- [130] M. Godec, P. M. Roth, and H. Bischof, "Hough-based tracking of non-rigid objects," in *ICCV*, D. N. Metaxas, L. Quan, A. Sanfeliu, and L. V. Gool, Eds., 2011, pp. 81–88.
- [131] L. Wen, D. Du, Z. Lei, S. Z. Li, and M. Yang, "JOTS: joint online tracking and segmentation," in *CVPR*, 2015, pp. 2226–2234.
- [132] H. Possegger, T. Mauthner, and H. Bischof, "In defense of color-based model-free tracking," in *CVPR*, 2015, pp. 2113–2120.
- [133] A. Adam, E. Rivlin, and I. Shimshoni, "Robust fragments-based tracking using the integral histogram," in *CVPR*, 2006, pp. 798–805.
- [134] G. Nebehay and R. P. Pflugfelder, "Clustering of static-adaptive correspondences for deformable object tracking," in *CVPR*, 2015, pp. 2784–2791.
- [135] D. Du, H. Qi, L. Wen, Q. Tian, Q. Huang, and S. Lyu, "Geometric hypergraph learning for visual tracking," vol. 47, no. 12, pp. 4182–4195, 2017.
- [136] J. Zhang, S. Ma, and S. Sclaroff, "MEEM: robust tracking via multiple experts using entropy minimization," in *ECCV*, D. J. Fleet, T. Pajdla, B. Schiele, and T. Tuytelaars, Eds., vol. 8694, 2014, pp. 188–203.
- [137] L. Wen, Z. Cai, Z. Lei, D. Yi, and S. Z. Li, "Robust online learned spatio-temporal context model for visual tracking," *TIP*, vol. 23, no. 2, pp. 785–796, 2014.
- [138] T. Zhang, S. Liu, N. Ahuja, M. Yang, and B. Ghanem, "Robust visual tracking via consistent low-rank sparse learning," *IJCV*, vol. 111, no. 2, pp. 171–190, 2015.
- [139] Y. Li and J. Zhu, "A scale adaptive kernel correlation filter tracker with feature integration," in *ECCV Workshops*, L. Agapito, M. M. Bronstein, and C. Rother, Eds., vol. 8926, 2014, pp. 254–265.
- [140] M. Danelljan, A. Robinson, F. S. Khan, and M. Felsberg, "Beyond correlation filters: Learning continuous convolution operators for visual tracking," in *ECCV*, 2016, pp. 472–488.
- [141] A. Lukezic, L. C. Zajc, and M. Kristan, "Deformable parts correlation filters for robust visual tracking," *IEEE Trans. Cybernetics*, vol. 48, no. 6, pp. 1849–1861, 2018.
- [142] K. Dai, D. Wang, H. Lu, C. Sun, and J. Li, "Visual tracking via adaptive spatially-regularized correlation filters," in *CVPR*, 2019, pp. 4670–4679.
- [143] C. Ma, J. Huang, X. Yang, and M. Yang, "Robust visual tracking via hierarchical convolutional features," *TPAMI*, vol. 41, no. 11, pp. 2709–2723, 2019.
- [144] C. Sun, D. Wang, H. Lu, and M. Yang, "Learning spatial-aware regressions for visual tracking," in *CVPR*, 2018, pp. 8962–8970.
- [145] Q. Wang, L. Zhang, L. Bertinetto, W. Hu, and P. H. S. Torr, "Fast online object tracking and segmentation: A unifying approach," in *CVPR*, 2019, pp. 1328–1338.
- [146] B. Chen, P. Li, C. Sun, D. Wang, G. Yang, and H. Lu, "Multi attention module for visual tracking," *PR*, vol. 87, pp. 80–93, 2019.
- [147] D. Ma, W. Bu, and X. Wu, "Multi-scale recurrent tracking via pyramid recurrent network and optical flow," in *BMVC*, 2018, p. 242.
- [148] A. Lukezic, T. Vojir, L. C. Zajc, J. Matas, and M. Kristan, "Discriminative correlation filter with channel and spatial reliability," in *CVPR*, 2017, pp. 4847–4856.
- [149] C. Ma, X. Yang, C. Zhang, and M. Yang, "Long-term correlation tracking," in *CVPR*, 2015, pp. 5388–5396.
- [150] M. Danelljan, G. Häger, F. S. Khan, and M. Felsberg, "Accurate scale estimation for robust visual tracking," in *BMVC*, 2014.
- [151] M. Danelljan, G. Häger, F. S. Khan, and M. Felsberg, "Learning spatially regularized correlation filters for visual tracking," in *ICCV*, 2015, pp. 4310–4318.
- [152] J. Choi, H. J. Chang, J. Jeong, Y. Demiris, and J. Y. Choi, "Visual tracking using attention-modulated disintegration and integration," in *CVPR*, 2016, pp. 4321–4330.
- [153] M. Danelljan, G. Häger, F. S. Khan, and M. Felsberg, "Discriminative scale space tracking," *TPAMI*, vol. 39, no. 8, pp. 1561–1575, 2017.
- [154] H. Fan and H. Ling, "Parallel tracking and verifying: A framework for real-time and high accuracy visual tracking," in *ICCV*, 2017, pp. 5487–5495.
- [155] C. Ma, J. Huang, X. Yang, and M. Yang, "Hierarchical convolutional features for visual tracking," in *ICCV*, 2015, pp. 3074–3082.
- [156] Q. Guo, W. Feng, C. Zhou, R. Huang, L. Wan, and S. Wang, "Learning dynamic siamese network for visual object tracking," in *ICCV*, 2017, pp. 1781–1789.
- [157] L. Bertinetto, J. Valmadre, J. F. Henriques, A. Vedaldi, and P. H. S. Torr, "Fully-convolutional siamese networks for object tracking," in *ECCV*, 2016, pp. 850–865.
- [158] J. Choi, H. J. Chang, T. Fischer, S. Yun, K. Lee, J. Jeong, Y. Demiris, and J. Y. Choi, "Context-aware deep feature compression for high-speed visual tracking," in *CVPR*, 2018, pp. 479–488.
- [159] L. Huang, X. Zhao, and K. Huang, "Got-10k: A large high-diversity benchmark for generic object tracking in the wild," *CoRR*, vol. abs/1810.11981, 2018.
- [160] M. Müller, A. Bibi, S. Giancola, S. Al-Subaihi, and B. Ghanem, "Trackingnet: A large-scale dataset and benchmark for object tracking in the wild," in *ECCV*, 2018, pp. 310–327.
- [161] E. Real, J. Shlens, S. Mazzocchi, X. Pan, and V. Vanhoucke, "Youtube-boundingboxes: A large high-precision human-annotated data set for object detection in video," in *CVPR*, 2017, pp. 7464–7473.
- [162] Z. Ying, G. Li, Y. Ren, R. Wang, and W. Wang, "A new low-light image enhancement algorithm using camera response model," in *ICCV Workshops*, 2017, pp. 3015–3022.
- [163] C. Zhang, S. Ge, Y. Hua, and D. Zeng, "Robust deep tracking with two-step augmentation discriminative correlation filters," in *ICME*, 2019, pp. 1774–1779.
- [164] G. Bhat, J. Johnander, M. Danelljan, F. S. Khan, and M. Felsberg, "Unveiling the power of deep tracking," in *ECCV*, 2018, pp. 493–509.
- [165] B. X. Chen and J. K. Tsotsos, "Fast visual object tracking with rotated bounding boxes," *CoRR*, vol. abs/1907.03892, 2019.
- [166] Z. Cai, L. Wen, Z. Lei, N. Vasconcelos, and S. Z. Li, "Robust deformable and occluded object tracking with dynamic graph," *TIP*, vol. 23, no. 12, pp. 5497–5509, 2014.
- [167] Z. Kalal, K. Mikolajczyk, and J. Matas, "Tracking-learning-detection," *TPAMI*, vol. 34, no. 7, pp. 1409–1422, 2012.
- [168] W. Tian and M. Lauer, "Joint tracking with event grouping and temporal constraints," in *AVSS*, 2017, pp. 1–5.
- [169] N. Wojke, A. Bewley, and D. Paulus, "Simple online and realtime tracking with a deep association metric," in *ICIP*, 2017, pp. 3645–3649.
- [170] H. Pirsiavash, D. Ramanan, and C. C. Fowlkes, "Globally-optimal greedy algorithms for tracking a variable number of objects," in *CVPR*, 2011, pp. 1201–1208.
- [171] N. M. Al-Shakarji, G. Seetharaman, F. Bunyak, and K. Palaniappan, "Robust multi-object tracking with semantic color correlation," in *AVSS*, 2017, pp. 1–7.
- [172] W. Tian and M. Lauer, "Fast cyclist detection by cascaded detector and geometric constraint," in *IEEE International Conference on Intelligent Transportation Systems*, 2015, pp. 1286–1291.
- [173] E. Bochinski, V. Eiselein, and T. Sikora, "High-speed tracking-by-detection without using image information," in *AVSS*, 2017, pp. 1–6.
- [174] D. Sun, X. Yang, M. Liu, and J. Kautz, "Pwc-net: Cnns for optical flow using pyramid, warping, and cost volume," in *CVPR*, 2018, pp. 8934–8943.
- [175] H. Ardö and M. Nilsson, "Multi target tracking by learning from generalized graph differences," *CoRR*, vol. abs/1908.06646, 2019.
- [176] K. Zhou, Y. Yang, A. Cavallaro, and T. Xiang, "Omni-scale feature learning for person re-identification," *CoRR*, vol. abs/1905.00953, 2019.
- [177] N. Wojke and A. Bewley, "Deep cosine metric learning for person re-identification," in *WACV*, 2018, pp. 748–756.
- [178] D. P. Bertsekas, "Auction algorithms for network flow problems: A tutorial introduction," *Comp. Opt. and Appl.*, vol. 1, no. 1, pp. 7–66, 1992.
- [179] A. Alahi, K. Goel, V. Ramanathan, A. Robicquet, F. Li, and S. Savarese, "Social LSTM: human trajectory prediction in crowded spaces," in *CVPR*, 2016, pp. 961–971.
- [180] E. Ilg, N. Mayer, T. Saikia, M. Keuper, A. Dosovitskiy, and T. Brox, "FlowNet 2.0: Evolution of optical flow estimation with deep networks," in *CVPR*, 2017, pp. 1647–1655.
- [181] L. Chen, H. Ai, Z. Zhuang, and C. Shang, "Real-time multiple people tracking with deeply learned candidate selection and person re-identification," in *ICME*, 2018, pp. 1–6.
- [182] G. Wang, Y. Wang, H. Zhang, R. Gu, and J. Hwang, "Exploit the connectivity: Multi-object tracking with trackletnet," in *ACM MM*, 2019.
- [183] W. Tian, M. Lauer, and L. Chen, "Online multi-object tracking using joint domain information in traffic scenarios," *TITS*, vol. 21, no. 1, pp. 374–384, 2020.

- [184] S. Sun, N. Akhtar, H. Song, A. Mian, and M. Shah, "Deep affinity network for multiple object tracking," *TPAMI*, 2019.
- [185] R. Hess and A. Fern, "Discriminatively trained particle filters for complex multi-object tracking," in *CVPR*, 2009, pp. 240–247.
- [186] L. Marchesotti, L. Marcenaro, G. Ferrari, and C. S. Regazzoni, "Multiple object tracking under heavy occlusions by using kalman filters based on shape matching," in *ICIP*, 2002, pp. 341–344.
- [187] S. H. Bae and K. Yoon, "Robust online multi-object tracking based on tracklet confidence and online discriminative appearance learning," in *CVPR*, 2014, pp. 1218–1225.
- [188] A. Bewley, Z. Ge, L. Ott, F. T. Ramos, and B. Upcroft, "Simple online and realtime tracking," in *ICIP*, 2016, pp. 3464–3468.
- [189] A. Andriyenko, K. Schindler, and S. Roth, "Discrete-continuous optimization for multi-target tracking," in *CVPR*, 2012, pp. 1926–1933.
- [190] A. Milan, S. Roth, and K. Schindler, "Continuous energy minimization for multitarget tracking," *TPAMI*, vol. 36, no. 1, pp. 58–72, 2014.
- [191] Y. Xiang, A. Alahi, and S. Savarese, "Learning to track: Online multi-object tracking by decision making," in *ICCV*, 2015, pp. 4705–4713.
- [192] L. Wen, Z. Lei, S. Lyu, S. Z. Li, and M. Yang, "Exploiting hierarchical dense structures on hypergraphs for multi-object tracking," *TPAMI*, vol. 38, no. 10, pp. 1983–1996, 2016.
- [193] L. Wen, D. Du, S. Li, X. Bian, and S. Lyu, "Learning non-uniform hypergraph for multi-object tracking," in *AAAI*, 2019, pp. 8981–8988.
- [194] S. Zhang, Y. Gong, J. Huang, J. Lim, J. Wang, N. Ahuja, and M. Yang, "Tracking persons-of-interest via adaptive discriminative features," in *ECCV*, B. Leibe, J. Matas, N. Sebe, and M. Welling, Eds., vol. 9909, 2016, pp. 415–433.
- [195] H. Zhou, W. Ouyang, J. Cheng, X. Wang, and H. Li, "Deep continuous conditional random fields with asymmetric inter-object constraints for online multi-object tracking," *TCSVT*, vol. 29, no. 4, pp. 1011–1022, 2019.
- [196] A. Sadeghian, A. Alahi, and S. Savarese, "Tracking the untrackable: Learning to track multiple cues with long-term dependencies," in *ICCV*, 2017, pp. 300–311.
- [197] A. Milan, S. H. Rezatofighi, A. R. Dick, I. D. Reid, and K. Schindler, "Online multi-target tracking using recurrent neural networks," in *AAAI*, 2017, pp. 4225–4232.
- [198] A. Maksai and P. Fua, "Eliminating exposure bias and loss-evaluation mismatch in multiple object tracking," *CoRR*, vol. abs/1811.10984, 2018.
- [199] P. Bergmann, T. Meinhardt, and L. Leal-Taixé, "Tracking without bells and whistles," in *ICCV*, 2019, pp. 941–951.
- [200] X. Zhou, V. Koltun, and P. Krähenbühl, "Tracking objects as points," *CoRR*, vol. abs/2004.01177, 2020.